THE ASTROPHYSICAL JOURNAL

AN INTERNATIONAL REVIEW OF SPECTROSCOPY AND ASTRONOMICAL PHYSICS

VOLUME 133 MARCH 1961 NUMBER 2

# THE ABILITY OF THE 200-INCH TELESCOPE TO DISCRIMINATE BETWEEN SELECTED WORLD MODELS

ALLAN SANDAGE
Mount Wilson and Palomar Observatories
Carnegie Institution of Washington, California Institute of Technology
*Received October 14, 1960; revised November 5, 1960*

## ABSTRACT

The present paper reviews several tests which can be performed to decide between world models. Each test is discussed in terms of the capabilities of the 200-inch Hale telescope. The tests include (1) the deviation from linearity of the red-shift–magnitude relation, (2) the galaxy-count–magnitude relation, (3) the angular-diameter–red-shift relation treated for both metric and isophotal diameters, and (4) the time scale. Selected exploding models of the Friedman type and the steady-state model are considered. The object of the tests is to determine observationally the deceleration parameter $q_0$. Once $q_0$ is known, the world model follows from equations given in Section I.

It appears possible to find $q_0$ from the magnitude–red-shift relation. At a red shift $(\Delta\lambda/\lambda_0)$ of $z = 0.5$, a difference of 0.9 mag. exists in the $[m, z]$ relation between a closed, elliptical universe with $q_0 = +1$ and the steady-state model with $q_0 = -1$. Such a difference can possibly be detected if the aperture effect for the measurement of intensities and if the Scott effect of observational selection can be allowed for. The value of $q_0$ is presently estimated to lie between 0 and +3. The most probable value is $q_0 = 1 \pm \frac{1}{2}$. The predictions of steady-state cosmology would appear to be inconsistent with present information.

The $N(m)$ relation for galaxy counts is derived for all models considered. Galaxy counts are insensitive to the model. At the limit of the 200-inch, an observational error of only $\Delta m_R = 0.28$ mag. can change the counts from indicating a closed universe with $q_0 = +1$ to an open, empty model with $q_0 = 0$. There seems to be no hope of finding $q_0$ from the $N(m)$ counts because the predicted differences between the models are too small compared with the known fluctuations of the distribution.

The angular diameters of clusters of galaxies and of galaxies themselves are discussed. The angular diameter subtended by a linear distance $y$ is shown to change with $z$ in a different way than the isophotal diameters. Both types of diameters are considered, and a test for $q_0$ seems to be possible with the 200-inch, but the test will be difficult and perhaps marginal

Equations for the time $t_0$ since the beginning of the expansion are derived. It is shown that $t_0$ is a function of the Hubble parameter $H_0$ and $q_0$ alone for exploding models with $\Lambda = 0$. The present value of $H_0$ and the age of the oldest stars are shown to be incompatible. If $q_0 = +1$, then $t_0 = 0.571\, H_0^{-1} = 7.42 \times 10^9$ years (assuming $H_0 = 75$ km/sec $10^6$ pc). However, the age of the oldest stars in our Galaxy is computed to be greater than $15 \times 10^9$ years if the most recent stellar models of Hazelgrove and Hoyle are used. These values are too uncertain to claim that exploding models with $\Lambda = 0$ are incorrect, but the data, as given, would so require. It is shown in the final section that exploding models of the Lemaitre-Eddington type approach asymptotically $q_0 = -1$ and are therefore like the steady-state model. In the limit both models predict the same $[m, z]$ and $[\theta, z]$ relations Consequently, tests of the type considered in this paper cannot decide between these particular models Appeal to the time independence of the steady-state model must then be made for a test. Appendix A gives the explicit equations for $N(m)$ for various $q_0$ values.

Renewed interest in the cosmological problem is evidenced by the number of recent papers which treat the fitting of observational data to predictions of the theory (Robertson 1955; McVittie 1956; Mattig 1958, 1959; Wheeler 1958; Davidson 1959; Hoyle 1959; etc.). The observational quantities which are available for comparison are (1) the apparent magnitude of galaxies, (2) the red shift, (3) the angular diameters of galaxies and of clusters of galaxies, and (4) galaxy counts. Differences in the relations are given by the several theories and provide the means of choosing that theory, if any, which best fits the real world. Unfortunately, the predicted differences become significantly large only when distances of the order of the radius of curvature of the universe are reached. A decision between the possible classes of models therefore cannot be made until observations are pushed near to, or perhaps even beyond, the telescopic limit of the 200-inch. The purpose of this paper is to (1) review the various theories, (2) express the theoretical predictions in terms of observational quantities only, and (3) determine whether detection of the second-order differences is within the reach of the 200-inch telescope. Because some of the theoretical equations are well known, parts of this paper may be considered as a review.

## I. THE BASIC EQUATIONS AND THE DECELERATION PARAMETER $q_0$

The elements of modern cosmological theory have been extensively treated by a number of people. Several of the more complete discussions are due to Robertson (1933, 1955, 1956), McCrae (1953), McVittie (1956), de Sitter (1933), and Bondi (1952). Reference has been made to these sources as a basis for the present paper.

Although, in principle, a problem such as the determination of the Riemannian curvature of space can be solved by appeal to geometry alone (by counting objects distributed uniformly in space and finding deviations from an $r^3$ increase), most cosmological problems require appeal to the field equations of general relativity which relate the intrinsic geometry of space to the energy content of the universe. And because observations of the deceleration of the red-shift rate can in principle give the energy content of the universe, we can obtain the components of the metric tensor by observations at the telescope. The present discussion traces the consequences of the original field equations of Einstein, as discussed by Friedman (1922) for the evolving cosmological models, and the field equations given by Hoyle for the steady-state models.

Astronomical observations are to be used to decide between the various special solutions of these field equations. It turns out that the large variety of possible world models makes a final decision between the models impossible because there are more parameters in the equations than can be determined observationally. Consequently, we restrict the bulk of the present review to those evolving models where the cosmological constant is zero, thus reducing one parameter and making a unique decision between the evolving models and the steady-state model possible in principle.

If we adopt the postulate that the universe is isotropic and homogeneous (the so-called cosmological principle), then the most general expression for line element is that given by Robertson (1929) and Walker (1936) as

$$ds^2 = c^2 dt^2 - R^2(t)\, du^2 . \tag{1}$$

Here $du$ represents an auxiliary three-space of constant Riemannian curvature and is a function of the dimensionless co-moving space co-ordinates and is independent of time. A more explicit form is given by equation (44). The function $R(t)$ is determined by introducing equation (1) into the Einstein field equations, giving the two well-known fundamental differential equations of the cosmological problem as

$$\frac{\dot{R}^2}{R^2} + \frac{2\ddot{R}}{R} + \frac{8\pi G p}{c^2} = -\frac{k c^2}{R^2} + \Lambda c^2 , \tag{2}$$

$$\frac{\dot{R}^2}{R^2} - \frac{8\pi G\rho}{3} = -\frac{kc^2}{R^2} + \frac{\Lambda c^2}{3}, \tag{3}$$

whose solution gives information on the geometrical history of the world (see, e.g., Robertson 1933, eq. [3.2]). Here $p$ is the isotropic hydrodynamic pressure of matter and radiation, $\rho$ is the density of matter and energy, $\Lambda$ is the cosmological constant, and $k/R^2$ is the Riemannian spatial curvature. The curvature can be either greater than, less than, or equal to zero, according to whether the space is closed, open, and Euclidean, or open and curved. The index $k$ takes values of $+1$, 0, or $-1$ for these three cases.

Equations (2) and (3) hold for all time and, in particular, hold for the present epoch of observation, denoted by the subscript zero. The equations can, without integration, be made to yield interesting results if we introduce the present value of the Hubble expansion parameter, $H_0$, and the present value of the deceleration parameter, $q_0$, both of which are observable. Following Robertson (1955) and Hoyle and Sandage (1956),

$$H_0 \equiv \frac{\dot{R}_0}{R_0}, \tag{4}$$

$$q_0 = -\frac{\ddot{R}_0}{R_0 H_0^2}. \tag{5}$$

Subtraction of equation (3) from equation (2) and treating those models with $\Lambda = 0$, gives

$$\frac{\ddot{R}_0}{R_0} + 4\pi G\left(\frac{\rho_0}{3} + \frac{p_0}{c^2}\right) = 0, \tag{6}$$

which reduces to

$$\rho_0 + \frac{3p_0}{c^2} = \frac{3H_0^2 q_0}{4\pi G} \tag{7}$$

by substitution of equation (5) in equation (6). This is the general equation for the mean density plus pressure of matter and radiation in the universe and becomes, upon substitution of $H_0 = 75$ km/sec $10^6$ pc (Sandage 1958),

$$\rho_0 + \frac{3p_0}{c^2} = 2.06 \times 10^{-29} q_0 \text{ gm/cm}^3. \tag{8}$$

Hence, if $q_0$ can be determined by observations of red shifts and magnitudes as in Section II, then $\rho_0 + 3p_0/c^2$ is known.

A second result is found by substitution of equation (4) in equation (3), which gives, for $\Lambda = 0$,

$$\frac{kc^2}{R_0^2} = \frac{8\pi G\rho_0}{3} - H_0^2, \tag{9}$$

which, when combined with equation (7), gives, for the spatial curvature at the present epoch,

$$\frac{kc^2}{R_0^2} = \frac{4\pi G}{3q_0}\left[\rho_0(2q_0 - 1) - \frac{3p_0}{c^2}\right]. \tag{10}$$

Note that this equation expresses one of the major themes of general relativity, namely, that the intrinsic geometry of space, expressed here by the spatial curvature $k/R_0^2$, is determined by the energy content of the universe as measured by the total density and pressure.

It is now of interest to estimate the values of $\rho_0$ and $p_0$ and thereby simplify equations (7), (8), and (10). The pressure $p_0$ is the sum of the pressure due to radiation, $aT_0^4/3$, and the pressure due to the random motions of the galaxies (given by the two-thirds of the energy density of random motions, which reduces to $\rho v^2$, where $v$ is the random radial velocity, observed to be less than 300 km/sec [Hubble 1936]). The density $\rho_0$ is the sum of the matter density $\rho_{0,m}$ and the matter equivalent of the radiation density given by $aT_0^4/c^2$, where $a$ is Stefan's constant. Consequently, equation (7) becomes

$$\rho_{0,m} + \frac{2aT_0^4}{c^2} + \frac{3\rho_{0,m}v_0^2}{c^2} = \frac{3H_0^2 q_0}{4\pi G}. \tag{11}$$

At the present epoch, $\rho_{0,m}$ of the *visible* matter is of the order of $10^{-31}$ gm/cm$^3$ (Hubble 1926; Whitford 1954; Oort 1958). The present radiation temperature of intergalactic space has never been properly estimated by summing the intensity of all the galaxies to the observable horizon, but it is unlikely that $T_0$ is greater than 3° K, which applies to interstellar space within our own Galaxy (Eddington 1930; Dunham 1939). Consequently, the radiation term, $aT_0^4/c^2$, at the present epoch is of the order of, or less than, $10^{-33}$ gm/cm$^3$, which is negligible compared with the observed matter density of $10^{-31}$ gm/cm$^3$. Likewise, the random-motion pressure term, $3\rho_{0,m}v^2/c^2$, is negligible compared with $\rho_{0,m}$. Therefore, at the present epoch we can equate $p_0$ to zero, and equations (7), (8), and (10) take the important simplified forms

$$\rho_0 = \frac{3H_0^2 q_0}{4\pi G} = 2.06 \times 10^{-29} q_0 \text{ gm/cm}^3, \tag{7', 8'}$$

$$\frac{kc^2}{R_0^2} = H_0^2 (2q_0 - 1), \tag{10'}$$

valid for a universe where radiation is negligible and matter pressure is zero.

We shall note in passing that equation (7′, 8′) predicts a density some 50 times the observed value of $\sim 10^{-31}$ gm/cm$^3$. This follows from the observed value of $q_0 \cong 1$. The reason for this discrepancy is not understood at present. If the cosmological theory with $\Lambda = 0$ is valid, it may mean that large amounts of non-luminous matter exist in space. (The theory can be made to give the observed low value of $10^{-31}$ gm/cm$^3$ if $\Lambda$ is made large and negative, keeping $q_0 = +1$ as observed. However, a negative cosmological constant seems unreasonable from general considerations and its introduction to save the phenomenon is rejected here.)

Equation (10′) relates the present radius of curvature of the universe with $H_0$ and $q_0$, both of which are shown in the next section to be observable. This equation shows that the limits of $q_0$ for the three possible values of $k$ are: $q_0 > \frac{1}{2}$ for $k = +1$ (closed, elliptical models); $q_0 = \frac{1}{2}$ for $k = 0$ (Euclidean geometry); $0 \leq q_0 < \frac{1}{2}$ for $k = -1$ (open, hyperbolic models). The lower limit for exploding models is $q_0 = 0$ for $k = -1$. This follows from equation (7) if $\rho_0 = 0$. Here the universe is empty. Further consequences of these equations are discussed by Hoyle and Sandage (1956).

The above system of equations is sufficient to obtain the magnitude, red shift, count, and angular size functions, and we could break off the discussion at this point to derive the results of Sections II and IV. However, for the time-scale problem it is important to consider the case where $p$ cannot be neglected; consequently, the following several paragraphs are added for later reference in Section V.

We cannot assume that the pressure is zero in the early history of the universe because the radiation term becomes important in equation (11) and, indeed, overwhelms the density term. In an adiabatic expansion the radiation density, $u$, decreases faster than does the matter density, $\rho$. General considerations show that $T$ varies as $R^{-1}$, while

$\rho$ varies as $R^{-3}$. Consequently, the radiation term varies as $R^{-4}$, which for small $R$ makes $aT^4/c^2$ larger than $\rho$ if we go far enough into the past. This domination of radiation over matter in the early phase of the expansion is an important feature emphasized first by Alpher (1948) and Alpher and Herman (1949). At a time far enough in the past when $aT^4/c^2 \gg \rho_m$, the entire density and pressure are effectively due to radiation alone and are equal to $\rho_0 = u/c^2$, $p_0 = u/3$. In this case equation (7) or (11) becomes

$$2u_0 = \frac{3H_0^2 q_0 c^2}{4\pi G}, \tag{12}$$

where $u = aT^4$. Equation (10) then becomes

$$\frac{k c^2}{R_0^2} = \frac{8\pi G u_0}{3 q_0 c^2}(q_0 - 1), \tag{13}$$

where the subscript zero again signifies that the values refer to the time of observation. Substitution of equation (12) in equation (13) gives the analogue of equation (10′) for a radiation-filled universe as

$$\frac{k c^2}{R_0^2} = H_0^2 (q_0 - 1), \tag{14}$$

a result which will be used in Section V.

Equation (14) shows that in a radiation-filled universe $q_0 > 1$ for $k = +1$, $q_0 = 1$ for $k = 0$, and $0 < q_0 < 1$ for $k = -1$, which is a different correspondence than that which holds for a matter-filled universe (cf. eq. [10′]).

## II. THE MAGNITUDE–RED-SHIFT RELATION

Perhaps the most important contact between theory and observation occurs at the apparent bolometric magnitude–red-shift relation. Beginning with Robertson's (1928) and Hubble's (1929) independent discovery of a linear relation between red shift and apparent magnitude, a series of observational studies emerged, due entirely to Hubble and Humason at Mount Wilson and to Mayall at Lick (Hubble and Humason 1931; Humason 1931; Hubble 1936*a*, 1936*b*, 1953; Humason 1936; Humason, Mayall, and Sandage 1956). All these studies showed that the relation between log $z$ and $m_{\text{bol}}$ is linear for red shifts less than $z = 0.15$ to within the accuracy of the data.

Robertson, Heckman, McVittie, and others approached the problem theoretically and showed that a linear relation between the *metric distance* $u$ and $z$ must exist at any given cosmic time for all models which obey the "cosmological principle," i.e., models which are homogeneous and isotropic. The difficulty with such a result is that the metric distance is not directly observed. Only apparent brightness of comparable sources can be measured at the telescope. However, Robertson showed in 1938 how $u$ and magnitude are related and thus gave the necessary connection to predict the $[m, z]$ relation from the $[u, z]$ relation.

A further complication arises which, as it turns out, provides the test between the cosmological models. Because of the finite speed of light, we cannot observe all parts of the universe at the same cosmic time. We see events at they happened a light travel time ago. Consequently, if the rate of expansion of the universe varies with time, we must expect to observe a deviation from linearity in the $[m, z]$ relation. The deviation will begin at the distance where the light travel time is large enough for a significant change in the expansion rate to have occurred. For example, if the expansion velocity $\dot{R}$ was larger in the past than it is today, we will observe that the distant galaxies will be receding faster than required by the linear rate $\dot{R}_0/R_0$, as determined from the nearby galaxies. And because different models predict different variations of $\dot{R}$ with time (i.e., $\ddot{R}$), the

deviation from linearity in the observed $[m, z]$ relation offers an observational test of the model.

The theory can be approached from two levels of complexity. The method of series of expansion followed by McVittie and by Robertson disclaims any knowledge of the functional form of $R(t)$ but requires knowledge of only the present-epoch value of $R_0(t_0)$ and its time derivatives, $\dot{R}_0$ and $\ddot{R}_0$. This is the kinematic approach and can yield series expansions for all the observed relations with no knowledge of equations (2) and (3). Here $R(t)$ is assumed to be sufficiently regular that a Taylor expansion from the present epoch $t_0$ into the past will give $R_1(t_1)$, where $t_1$ is the time of photon emission from any galaxy. The predicted $[m, z]$ relations are thus general. Heckman (1942), Robertson (1955), and McVittie (1956) derive in this way the relation

$$m_{\text{bol}} = 5 \log z + 1.086\,(1 - q_0)\, z + \ldots + \text{const.}\,, \tag{15}$$

correct to the first order in $z$. The deceleration parameter $q_0$ can therefore be found if the necessary observations of $m$ and $z$ are available.

The second approach introduces the field equations at the start, so that the functional form of $R(t)$ is known immediately by integrating equation (3). The method is less general than that of the series expansion because we must now assume the field equations. Nevertheless, the advantage is substantial because a particular value of $q_0$ is immediately identified with a particular world model through equation (10′). This cannot be done without the use of equations (2) and (3). In this connection it should be pointed out that the field equations must also be used in the series expansion method to determine the meaning of $q_0$ in terms of the spatial curvature $k/R_0^2$ and the density $\rho_0$ of the model. Therefore, the two methods differ only in the place of introduction of equation (3) for $R(t)$—that is, either before or after some form of equation (15) has been derived.

In what follows we adopt the second approach, which has the ultimate advantage that the $[m, z]$ relation is obtained in closed form rather than as a series expansion valid for $z < 1$ only. The theory proceeds as follows.

The metric distance of a galaxy which emits photons at time $t_1$ that arrive at the observer at time $t_0$ is

$$u = c \int_{t_1}^{t_0} \frac{dt}{R(t)}\,, \tag{16}$$

which follows from equation (1) because photons move along the null geodesic $ds = 0$.

If the galaxy in question is of total luminosity $L$, then, at the time of observation $t_0$, the apparent bolometric luminosity will be (Robertson 1938),

$$l = \frac{L}{4\pi R_0^2 \sigma^2(u)\,(1 + z)^2}\,. \tag{17}$$

The factor $4\pi R_0^2 \sigma^2(u)$ measures the area of the radiation wave front advancing from the particular galaxy and, because of the non-Euclidean geometry for $k = \pm 1$, is not equal to $4\pi R^2 u^2$. By use of the metric it is found that $\sigma(u) = u$ for $k = 0$, is $\sin u$ for $k = +1$, and is $\sinh u$ for $k = -1$ (see Sec. IV, eq. [47], for the well-known derivation).

Equations (16) and (17), together with

$$1 + z = \frac{R_0}{R_1}\,, \tag{18}$$

are now sufficient to obtain the $[m, z]$ relation.

The simplest example is provided by the steady-state model where $k = 0$ and $\sigma(u) =$

$u$. For this model the Hubble expansion parameter $H \equiv \dot{R}/R$ is required to be independent of time, which gives

$$R(t) = B e^{Ht}, \tag{19}$$

where $B$ is a constant.

Substitution of equation (19) in equation (16) and using equation (19) to simplify gives

$$u = \frac{c}{H}\left(\frac{1}{R_1} - \frac{1}{R_0}\right). \tag{20}$$

Using equation (18) to eliminate $R_1$ gives

$$u = \frac{c\,z}{HR_0}, \tag{21}$$

which, when substituted in equation (17), remembering that $k = 0$ and $\sigma(u) = u$, gives

$$l_{\text{bol}} = \frac{LH_0^2}{4\pi c^2 z^2 (1+z)^2}. \tag{22}$$

Converting equation (22) into astronomical magnitudes gives

$$m_{\text{bol}} = 5 \log z + 5 \log (1+z) + C, \tag{23}$$

which is the $[m, z]$ relation in closed form for the steady-state model. The "constant" contains $L$ and $H_0$ and is constant only if $L$ is assumed to be the same for all galaxies in the sample under observation.

In a similar way the $[m, z]$ relations for evolving models with $\Lambda = 0$ have been obtained by Mattig (1958), where $R(t)$ needed in equation (16) is found by integrating equation (3). By an elegant reduction, Mattig shows that, for all models with $q_0 > 0$,

$$m_{\text{bol}} = 5 \log \frac{1}{q_0^2}\{ q_0 z + (q_0 - 1)[\sqrt{(1 + 2 q_0 z)} - 1] \} + C. \tag{24}$$

For the special case of $q_0 = 0$,

$$m_{\text{bol}} = 5 \log z \left(1 + \frac{1}{2} z\right) + C. \tag{25}$$

The constant $C$ in equations (23), (24), and (25) can be found by fitting the equations to the available observations at bright magnitudes. The observations of interest for cosmology are usually made on members of clusters of galaxies, because in such clusters we can sample a definite part of the general luminosity function of galaxies and can thereby better restrict the study to those galaxies of nearly the same intrinsic luminosity. Furthermore, because the brightest galaxies in clusters have brighter absolute magnitudes than the average field galaxy, cluster galaxies will be brighter than field galaxies for a given red shift. In the study of Humason, Mayall, and Sandage (1956) the relation between $z$ and the corrected $P$ or $V$ magnitude for the first brightest cluster galaxy was found to be

$$\begin{aligned} m_v - k_v &= 5 \log z + 20.676, \\ m_p - k_p &= 5 \log z + 21.576, \end{aligned} \qquad \text{for } z \ll 1. \tag{26}$$

The $k$ term corrects the observed heterochromatic $m_p$ or $m_v$ magnitude for the photometric effect of red-shifting the energy distribution curve for galaxies through the

respective filter band (HMS, Appendix B). It is obvious that $m_{bol}$ in equations (23), (24), and (25) is equal to $m_i - k_i$ to within an additive constant (which is $\Delta m_{bol}$) and this additive constant can be absorbed into the constant term. In what follows we therefore give the relations in terms of $m_i - k_i$, where $m_i$ is the heterochromatic magnitude actually observed at the telescope in bands pass $i$.

In future observations a red band pass with cutoff wave lengths of about 6200 A and 7500 A will undoubtedly be used, because, for $z < \frac{1}{2}$, the $k_R$ will be close to zero for the entire range of $z$. Hence we compute the relations for a red-magnitude system denoted by $m_R$ and defined approximately by an S20 photocathode with a Schott RG 2 filter or by an Eastman 103*a*-F plate plus the RG2 filter. For such a system we can assume for the present purposes that color indices $m_p - m_R$ will be related to $m_p - m_v$ by an approximate transformation $m_p - m_R \cong 1.5\,(m_p - m_v)$. And because the normal color indices of the E galaxies in clusters are about $m_p - m_v \cong 0.87$, the color index $m_p - m_R$ will be close to 1.31. Consequently, the expected equation for $m_R$ magnitudes derived from equation (26) is

$$m_R - k_R = 5 \log z + 20.266 \qquad (z \ll 1)\,. \tag{27}$$

Equations (23), (24), and (25) then become

$$m_R - k_R = 5 \log z\,(1 + z) + 20.266 \tag{23'}$$

for the first brightest cluster galaxy in the SS model;

$$m_R - k_R = 5 \log q_0^{-2}\{q_0 z + (q_0 - 1)[\sqrt{(1 + 2 q_0 z)} - 1]\} + 20.266 \tag{24'}$$

for the first brightest cluster galaxy in evolving models with $q_0 > 0$; and

$$m_R - k_R = 5 \log z\left(1 + \frac{z}{2}\right) + 20.266 \tag{25'}$$

for the evolving model with $q_0 = 0$.

These functions are given in Table 1 with $m_R - k_R$ as the independent variable ranging from eighth to twenty-third magnitude. The last few tabulated values are well beyond the photographic range of the 200-inch, which is estimated to be $m_R \approx 23$. In making the calculation, it is convenient to treat the magnitude as the independent variable and $z$ as the unknown. Solving equations (23), (24), and (25) for $z$ gives

$$1 + z = \frac{1 + \sqrt{(1 + 4A)}}{2} \qquad \text{for } q_0 = -1 \text{ (SS)}\,, \tag{28}$$

$$1 + z = q_0(1 + A) - (q_0 - 1)\sqrt{(1 + 2A)} \qquad \text{for } q_0 \geq 0\,,$$

where

$$A \equiv 10^{0.2(m_R - k_R - C)}\,. \tag{29}$$

These equations show that $z$ is a function of $q_0$ and $A$ alone. Consequently, Table 1 might be called universal in the sense that if the $C$ value of equations (23), (24), and (25) is changed either by new observations or by a change in the wave length of the pass band, Table 1 need not be recomputed. However, the tabulated $1 + z$ values will refer to a different magnitude given by $C$ (new) $-20.266$. For example, if we wish $1 + z$ as a function of $m_v - k_v$ rather than $m_R - k_R$, we change the argument of Table 1 by $20.676 - 20.266 = 0.41$ mag., found by comparing equations (26) and (27).

The $[m_R - k_R, z, q_0]$ relation from Table 1 is plotted in Figure 1, which shows that significant differences exist well within the observational range of the 200-inch telescope between models with different $q_0$ values. If observations of sufficient precision can be made, a decision between the models may be possible. It is interesting to note (cf. eq.

TABLE 1

THE REDSHIFT-MAGNITUDE RELATION FOR THE FIRST RANKED CLUSTER GALAXY*

| $m_R - k_R$ | A | $q_0 = -1$ | | $q_0 = 0$ | | $q_0 = 0.5$ | | $q_0 = 1$ | |
|---|---|---|---|---|---|---|---|---|---|
| | | 1 + z | log c z | 1 + z | log c z | 1 + z | log c z | 1 + z | log c z |
| 8.0 | 0.0035221 | 1.003510 | 3.0224 | 1.003516 | 3.0232 | 1.003519 | 3.0235 | 1.003522 | 3.0239 |
| 8.5 | .0044340 | 1.004415 | 3.1220 | 1.004424 | 3.1230 | 1.004429 | 3.1234 | 1.004434 | 3.1239 |
| 9.0 | .0055821 | 1.005551 | 3.2215 | 1.005567 | 3.2227 | 1.005574 | 3.2233 | 1.005582 | 3.2239 |
| 9.5 | .0070275 | 1.006979 | 3.3209 | 1.007003 | 3.3224 | 1.007015 | 3.3232 | 1.007027 | 3.3239 |
| 10.0 | .0088471 | 1.008770 | 3.4201 | 1.008808 | 3.4220 | 1.008828 | 3.4230 | 1.008847 | 3.4239 |
| 10.5 | .0111378 | 1.011016 | 3.5192 | 1.011076 | 3.5215 | 1.011107 | 3.5227 | 1.011138 | 3.5239 |
| 11.0 | .0140217 | 1.013830 | 3.6180 | 1.013925 | 3.6209 | 1.013973 | 3.6224 | 1.014022 | 3.6239 |
| 11.5 | .0176522 | 1.017351 | 3.7165 | 1.017499 | 3.7201 | 1.017576 | 3.7220 | 1.017652 | 3.7239 |
| 12.0 | .0222229 | 1.021750 | 3.8146 | 1.021981 | 3.8192 | 1.022102 | 3.8216 | 1.022223 | 3.8239 |
| 12.5 | .0279769 | 1.027235 | 3.9123 | 1.027596 | 3.9180 | 1.027786 | 3.9210 | 1.027977 | 3.9239 |
| 13.0 | .0352209 | 1.034061 | 4.0094 | 1.034622 | 4.0165 | 1.034921 | 4.0202 | 1.035221 | 4.0239 |
| 13.5 | .0443404 | 1.042531 | 4.1058 | 1.043399 | 4.1149 | 1.043870 | 4.1193 | 1.044340 | 4.1239 |
| 14.0 | .0558213 | 1.053011 | 4.2015 | 1.054345 | 4.2123 | 1.055083 | 4.2181 | 1.055821 | 4.2239 |
| 14.5 | .0702749 | 1.065928 | 4.2962 | 1.067965 | 4.3094 | 1.069120 | 4.3167 | 1.070275 | 4.3239 |
| 15.0 | .0884708 | 1.081782 | 4.3898 | 1.084869 | 4.4059 | 1.086670 | 4.4150 | 1.088471 | 4.4239 |
| 15.5 | .111378 | 1.101147 | 4.4821 | 1.105783 | 4.5015 | 1.108580 | 4.5129 | 1.111378 | 4.5239 |
| 16.0 | .140217 | 1.124673 | 4.5729 | 1.131563 | 4.5963 | 1.135890 | 4.6103 | 1.140217 | 4.6239 |
| 16.5 | .176522 | 1.153086 | 4.6621 | 1.163204 | 4.6898 | 1.169863 | 4.7072 | 1.176522 | 4.7239 |
| 17.0 | .222229 | 1.187189 | 4.7494 | 1.201856 | 4.7822 | 1.212043 | 4.8036 | 1.222229 | 4.8239 |
| 17.5 | .279769 | 1.227852 | 4.8348 | 1.248815 | 4.8730 | 1.264292 | 4.8992 | 1.279769 | 4.9239 |
| 18.0 | .352209 | 1.276021 | 4.9181 | 1.305534 | 4.9622 | 1.328871 | 4.9941 | 1.352209 | 5.0239 |
| 18.5 | .443404 | 1.332709 | 4.9992 | 1.373611 | 5.0495 | 1.408508 | 5.0883 | 1.443404 | 5.1239 |
| 19.0 | .558213 | 1.399007 | 5.0781 | 1.454794 | 5.1349 | 1.506504 | 5.1817 | 1.558213 | 5.2239 |
| 19.5 | .702749 | 1.476089 | 5.1548 | 1.550967 | 5.2182 | 1.626858 | 5.2743 | 1.702749 | 5.3239 |
| 20.0 | 0.884708 | 1.565227 | 5.2293 | 1.664156 | 5.2994 | 1.774432 | 5.3661 | 1.884708 | 5.4239 |
| 20.5 | 1.11378 | 1.667810 | 5.3018 | 1.796541 | 5.3783 | 1.955161 | 5.4572 | 2.11378 | 5.5239 |
| 21.0 | 1.40217 | 1.785368 | 5.3722 | 1.950472 | 5.4551 | 2.17632 | 5.5476 | 2.40217 | 5.6239 |
| 21.5 | 1.76522 | 1.919584 | 5.4407 | 2.12848 | 5.5296 | 2.44685 | 5.6375 | 2.76522 | 5.7239 |
| 22.0 | 2.22229 | 2.072352 | 5.5075 | 2.33336 | 5.6021 | 2.77783 | 5.7270 | 3.22229 | 5.8239 |
| 22.5 | 2.79769 | 2.245763 | 5.5726 | 2.56815 | 5.6725 | 3.18292 | 5.8162 | 3.79769 | 5.9239 |
| 23.0 | 3.52209 | 2.442187 | 5.6361 | 2.83623 | 5.7410 | 3.67916 | 5.9051 | 4.52209 | 6.0239 |

TABLE 1 -continued

| $m_R - k_R$ | A | $q_0 = 2.5$ | | $q_0 = 5$ | | $q_0 = 8.5$ | | $q_0 = 13$ | |
|---|---|---|---|---|---|---|---|---|---|
| | | 1 + z | log c z | 1 + z | log c z | 1 + z | log c z | 1 + z | log c z |
| 8.0 | 0.0035221 | 1.003531 | 3.0250 | 1.003546 | 3.0269 | 1.003569 | 3.0317 | 1.003599 | 3.0333 |
| 8.5 | .0044340 | 1.004449 | 3.1254 | 1.004473 | 3.1277 | 1.004507 | 3.1310 | 1.004551 | 3.1352 |
| 9.0 | .0055821 | 1.005605 | 3.2257 | 1.005645 | 3.2288 | 1.005698 | 3.2328 | 1.005769 | 3.2382 |
| 9.5 | .0070275 | 1.007065 | 3.3262 | 1.007125 | 3.3299 | 1.007212 | 3.3352 | 1.007321 | 3.3417 |
| 10.0 | .0088471 | 1.008906 | 3.4268 | 1.009002 | 3.4315 | 1.009138 | 3.4380 | 1.009313 | 3.4462 |
| 10.5 | .0111378 | 1.011229 | 3.5275 | 1.011383 | 3.5334 | 1.011598 | 3.5415 | 1.011874 | 3.5517 |
| 11.0 | .0140217 | 1.014167 | 3.6284 | 1.014409 | 3.6358 | 1.014749 | 3.6459 | 1.015186 | 3.6586 |
| 11.5 | .0176522 | 1.017881 | 3.7295 | 1.018265 | 3.7387 | 1.018801 | 3.7513 | 1.019490 | 3.7669 |
| 12.0 | .0222229 | 1.022585 | 3.8309 | 1.023189 | 3.8424 | 1.024035 | 3.8580 | 1.025122 | 3.8772 |
| 12.5 | .0279769 | 1.028548 | 3.9327 | 1.029500 | 3.9469 | 1.030113 | 3.9559 | 1.032547 | 3.9896 |
| 13.0 | .0352209 | 1.036120 | 4.0349 | 1.037618 | 4.0525 | 1.039716 | 4.0761 | 1.042413 | 4.1046 |
| 13.5 | .0443404 | 1.045753 | 4.1375 | 1.048108 | 4.1593 | 1.051404 | 4.1881 | 1.055642 | 4.2225 |
| 14.0 | .0558213 | 1.058036 | 4.2408 | 1.061728 | 4.2676 | 1.066897 | 4.3025 | 1.073542 | 4.3437 |
| 14.5 | .0702749 | 1.073739 | 4.3448 | 1.079513 | 4.3776 | 1.087597 | 4.4196 | 1.097990 | 4.4683 |
| 15.0 | .0884708 | 1.093873 | 4.4497 | 1.102877 | 4.4894 | 1.115482 | 4.5396 | 1.131687 | 4.5967 |
| 15.5 | .111378 | 1.119771 | 4.5555 | 1.133758 | 4.6034 | 1.153341 | 4.6628 | 1.178519 | 4.7288 |
| 16.0 | .140217 | 1.153198 | 4.6624 | 1.174835 | 4.7197 | 1.205124 | 4.7981 | 1.244069 | 4.8646 |
| 16.5 | .176522 | 1.196499 | 4.7705 | 1.229793 | 4.8385 | 1.276408 | 4.9187 | 1.336336 | 5.0039 |
| 17.0 | .222229 | 1.252788 | 4.8800 | 1.303721 | 4.9596 | 1.375026 | 5.0512 | 1.466704 | 5.1462 |
| 17.5 | .279769 | 1.326200 | 4.9906 | 1.403587 | 5.0831 | 1.511926 | 5.1863 | 1.651221 | 5.2908 |
| 18.0 | .352209 | 1.422222 | 5.1027 | 1.538911 | 5.2086 | 1.702274 | 5.3236 | 1.912314 | 5.4373 |
| 18.5 | .443404 | 1.548093 | 5.2160 | 1.722575 | 5.3360 | 1.966849 | 5.4625 | 2.28092 | 5.5846 |
| 19.0 | .558213 | 1.713341 | 5.3304 | 1.971889 | 5.4647 | 2.33385 | 5.6022 | 2.79924 | 5.7322 |
| 19.5 | .702749 | 1.930422 | 5.4458 | 2.30988 | 5.5943 | 2.84111 | 5.7422 | 3.52413 | 5.8792 |
| 20.0 | .884708 | 2.21554 | 5.5619 | 2.76691 | 5.7243 | 3.53885 | 5.8818 | 4.53133 | 6.0251 |
| 20.5 | 1.11378 | 2.58964 | 5.6784 | 3.38274 | 5.8542 | 4.49307 | 6.0203 | 5.92065 | 6.1691 |
| 21.0 | 1.40217 | 3.07972 | 5.7951 | 4.20896 | 5.9835 | 5.78991 | 6.1574 | 7.82255 | 6.3111 |
| 21.5 | 1.76522 | 3.72033 | 5.9117 | 5.31217 | 6.1118 | 7.54075 | 6.2928 | 10.4061 | 6.4505 |
| 22.0 | 2.22229 | 4.55568 | 6.0280 | 6.77800 | 6.2389 | 9.88925 | 6.4260 | 13.8894 | 6.5874 |
| 22.5 | 2.79769 | 5.64200 | 6.1438 | 8.71586 | 6.3645 | 13.0193 | 6.5570 | 18.5522 | 6.7214 |
| 23.0 | 3.52209 | 7.05088 | 6.2589 | 11.2655 | 6.4885 | 17.1661 | 6.6857 | 24.7524 | 6.8528 |

*The tabulated magnitudes are for the red system described in the test. The relation for the usual visual system $m_V - k_V$ can be found by changing the argument by 0.41 mag., that is, the redshifts tabulated for $m_R - k_R = 8.0$ are the same as for $m_V - k_V = 8.41$.

[24′]) that the model with $q_0 = +1$ is the only one which predicts a strictly linear magnitude–log red-shift relation. Contrary to general belief, there is nothing special about this linear case other than the unique value of $q_0$ which is required.

Figure 1 shows that the magnitude difference between the steady-state model ($q_0 = -1$) and the exploding Euclidean case ($q_0 = \frac{1}{2}$) is 0.7 mag. for a red shift of $z = 0.5$. It should be noted that red shifts of $z = 0.5$ *can* be determined with the 200-inch prime-focus spectrograph (Minkowski 1960), although conditions must be nearly perfect.

A difference of 0.7 mag. can be detected if the effects of different measuring apertures in the photometric equipment can be eliminated (see HMS 1956, Appendix A). This is not an easy problem because, due to the effects of the red shift itself, the angular diameter which contains the same fraction of the total luminosity for nearby and distant galaxies is not a simple function of apparent magnitude. The necessary equations are derived in Section IV of the present paper.

Furthermore, the so-called "Scott effect" of observational selection must be eliminated from the clusters of galaxies chosen to define the [$m$, $z$] relation of Figure 1. Miss Scott (1956) assumes that the very distant galaxies will, on the average, be of higher intrinsic luminosity than those nearby, simply because in selecting clusters for study near the plate limit the richest clusters will be preferred. But this effect of observational

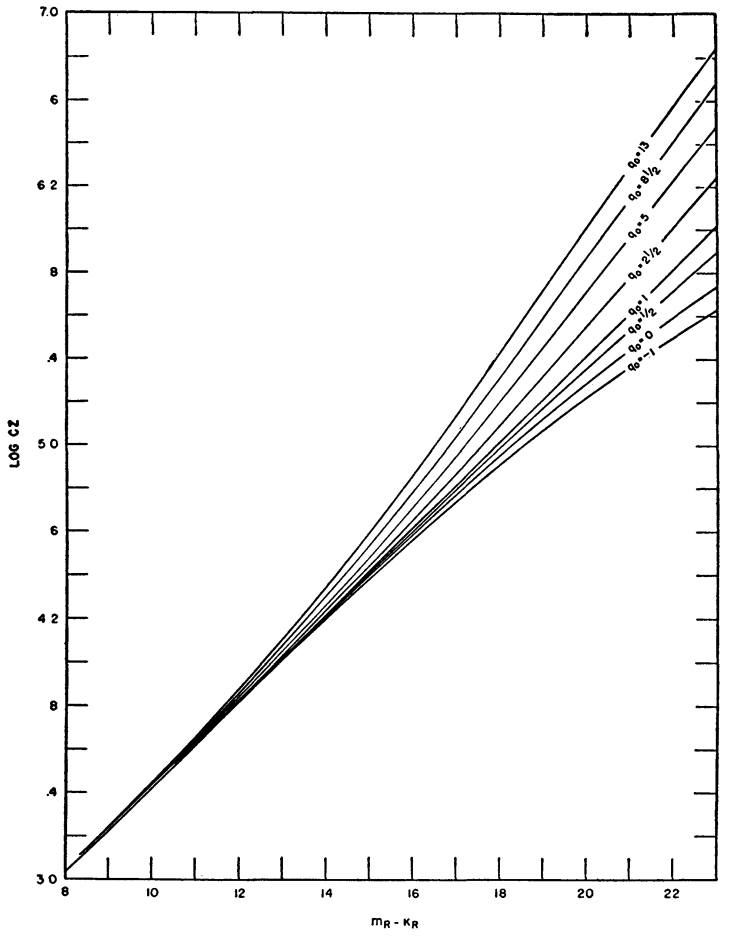


FIG 1.—The red-shift–magnitude relation for various values of the deceleration parameter. The abscissa is on a red magnitude system defined in the text The curves have been normalized to agree with the observations at bright magnitudes.

selection depends very much on the form of the luminosity function $\phi(M)$ for galaxies in clusters. Miss Scott assumes that, given two clusters of richness $N_1$ and $N_2$ with $N_1 > N_2$, the absolute luminosity of the brightest galaxy $G_1$ will be brighter than $G_2$ according to various models for $\phi(M)$. The observational data now at hand seem to suggest, however, that there is an upper limit to the luminosity of galaxies in clusters and this upper limit is reached when the membership of the group is greater than about 30 members—that is, $M_1 \cong M_2$ for $N_1 > N_2$ if $N_2 > 30$. This is shown by Table XI of HMS (1956) for groups where the first brightest galaxies of groups with only 30 members are about as bright as the brightest galaxies of rich clusters such as the Coma Cluster or the Corona Borealis Cluster. These data therefore suggest that the assumptions made by Miss Scott may be unrealistic in actual fact. But further work is needed by studies of $\phi(M) = f(N)$, such as that currently being carried out by Abell. The Scott effect, if it exists, can presumably be allowed for.

Finally, the observational test is plagued with the evolutionary problem of galaxies. The more distant galaxies will shine with the absolute luminosity which they had a light travel time ago, and if $L(\lambda) = f(\text{time})$, then appropriate evolutionary corrections must be applied to the observed magnitudes. The theory of evolution of individual stars is now on a much sounder basis than it was 10 years ago. Because of this, a theory for the evolution of the entire galactic system appears to be near at hand (Salpeter 1959; Schmidt 1959; van den Bergh 1957). Once $dL/dt$ is known from such a theory, the $[m, z]$ relation of Table 1 can be corrected for evolutionary effects by equations given by Robertson (1955). It therefore appears that the $[m, z]$ relation can decide between the simple models if red shift and magnitude observations of many clusters are obtained to $z \cong 0.5$.

There are two determinations of $q_0$ presently available in the literature, both of which refer to the case $dL/dt = 0$, i.e. evolution is neglected. Humason, Mayall, and Sandage's data for 18 clusters require $q_0 \cong +2.45 \pm 0.8$, a result which follows from Table XIV and equation (3) of their paper (1956); i.e., it is shown that $1.086\ (1 - q_0) = -1.976 \pm 0.895$ for the $m_v$ data and $1.086\ (1 - q_0) = -1.180 \pm 0.875$ for the $m_p$ data. Averaging the two values gives $\bar{q}_0 \cong 2.45 + 0.8$. The individual cluster data obtained from Table XIII of HMS are shown in Figure 2, together with the theoretical $[m_v - k_v, z]$ relation obtained from Table 1, but with the argument shifted by 0.41 mag., as already explained. The plotted points are correctly positioned in magnitude only insofar as the $k_v$ correction adopted from Appendix B of HMS is correct. However, it is known that the $I(\lambda)$-curve for M32 (Stebbins and Whitford 1948) used to obtain $k_v$ must be wrong because the $k_i$ values computed from this curve lead directly to the Stebbins-Whitford effect, which, according to unpublished measurements by Whitford (1956) and by Code (1959), does not exist as was once believed. Most of the original error in the M32 data can apparently be traced to the poor spectral resolution of the wide band passes used in the six-color photometry. Consequently, the value of $q_0 = 2.5 \pm 1$ obtained from Figure 2 is highly provisional, not only because of the uncertainty in the $k_v$ term but also because the scatter of the points in Figure 2 is larger than the difference in $q_0$ which we are after.

A recent determination of $q_0$ by Baum uses a more refined photometric technique, in which the $k$ term does not enter. By eight-color photometry Baum constructs the $I(\lambda)$-curve and reads the $\Delta$ mag. at any desired $\lambda$ for all cluster objects (Baum 1957). Baum's 1957 results gave $q_0 = 1 \pm \frac{1}{2}$ with the Euclidean value of $q_0 = \frac{1}{2}$ as distinctly possible. Baum's results undoubtedly have higher weight than those of HMS, and it seems quite clear that $q_0$ cannot be greater than 3 and likely lies between 2 and 0, again on the assumption that $dL/dt = 0$ over the range of times involved. This result already restricts the range of expected differences in the three tests of $[m, z]$, $[\log N(m), m]$, and $[\theta, z]$ discussed here and in the following two sections.

Finally, it is of interest to note where Minkowski's critical cluster (Minkowski 1960) lies in the $[m, z]$ plot. On two spectrograms of a galaxy taken with the prime-focus

spectrograph at the 200-inch telescope centered on radio source 3C 295, Minkowski identified $\lambda_0 = 3727$ [O II] in emission but red-shifted by $z = 0.46$. This galaxy was of about twenty-first visual magnitude. This red-shift value is shown as an arrow in Figure 2, together with arrows for Baum's values of $z = 0.29$ and $z = 0.35$ for the clusters discovered in 1956 by Humason and Sandage by inspection of the red 48-inch Schmidt plates for faint smudges. Baum has obtained preliminary photometric data (1960) for these three distant clusters. The data (not shown) suggest that $q_0$ is equal to or slightly greater than 1. The predictions of the steady-state theory, therefore, appear to be inconsistent with these data if the Scott effect is neglected and if $dL/dt = 0$. Because the red-shift–magnitude relation appears to be the best of the four tests discussed in this paper, refinement of this $q_0$ value undoubtedly will be one of the major problems to be studied with the 200-inch telescope in the next few years. New observations and a refined theory of the evolution of the light of galaxies will be required.

## III. THE COUNT-MAGNITUDE RELATION

If galaxies are distributed uniformly in space, counts to successive limits of parameter distance $u$ will yield numbers proportional to the volume inclosed within $u$. And, because volumes in Riemannian space vary either slower or faster than $u^3$, according to whether

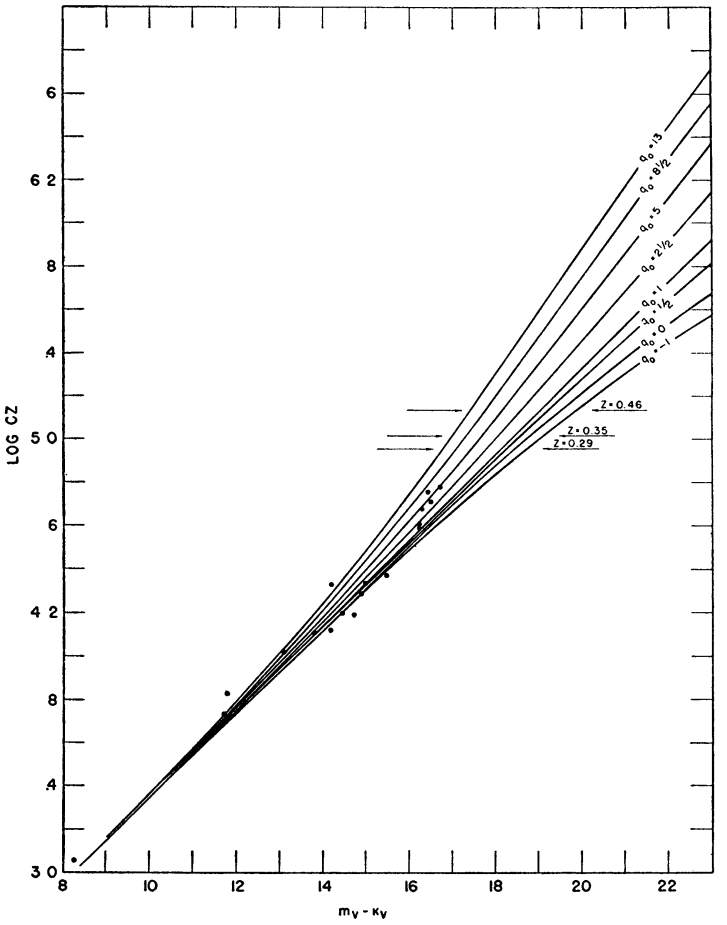


FIG. 2 —The theoretical red-shift–magnitude relation. Magnitudes are on the standard $V$ system, Data for 18 clusters of galaxies are plotted as given by Humason, Mayall, and Sandage Arrows are placed at the observed red-shift values for three distant clusters whose magnitudes are not yet available.

$k$ is $+1$ or $-1$, a determination of the spatial curvature is possible in principle. Observationally, we do not count galaxies to successive limits of $u$ but rather to successive limits of apparent magnitude where the connection between $u$ and apparent luminosity is given by equation (17).

Let $N(m)$ be the number of galaxies per square degree brighter than apparent magnitude $m$; $N(m)$ will be the number of galaxies contained within the volume inclosed by $u$ where $u = f(m)$. Robertson (1955) has given a series expansion for the derivative $d(ln\ N)/dm = f(q_0, z)$ which can be integrated by use of the $m = f(q_0, z)$ relations of equations (23), (24), and (25) to give a series expansion for $N(m)$. These equations will not be reproduced here because the approximations break down near the telescopic limit of the 200-inch telescope where $z \geq 1$ for the field galaxies. It can be shown that at a red magnitude $m_R - k_R = 21.0$, which, as we shall see, corresponds to an average red shift of $z = 0.41$ for field galaxies, the series expansion approximation for $\log N(m)$ to terms of order $z^2$ deviates from the exact relation by 1 per cent. At $m_R - k_R = 23$, which corresponds to $z = 0.87$, the approximation is off by 6 per cent, and beyond $m_R - k_R \cong 24$, where $z = 1$, the approximation is invalid. And because we eventually wish to compute

$$\lim_{m \to \infty} \log N(m)$$

to estimate the cosmic light, we require exact relations for $N(m)$ rather than series expansions in $z$.

Many authors have given exact equations for $N(u)$ for evolving models which obey equations (1), (2), and (3) with $\Lambda = 0$. Mattig's (1959) equations are the most convenient for computation and will be followed here. Let $n$ be the number of galaxies per unit volume, $Q$ be the number of square degrees in the sky, and assume, for the moment, that all galaxies have the same intrinsic luminosity $L$. The $N(m)$ is given by

$$N(m) = \frac{2\pi n}{QH_0^3} \begin{cases} (1 - 2q_0)^{-3/2} [P\sqrt{(1+P^2)} - \text{arc sinh}\, P] & (k = -1) \\ (2q_0 - 1)^{-3/2} [\text{arc sin}\, P - P\sqrt{(1-P^2)}] & (k = +1), \end{cases} \tag{30}$$

where

$$P = \frac{A\sqrt{[k(2q_0 - 1)]}}{q_0(1+A) - (q_0 - 1)\sqrt{(1+2A)}} \qquad \text{for } k = \pm 1 \tag{31}$$

and where $A$ is a function of apparent magnitude given by equation (29). For the Euclidean case of $k = 0$, $N(m)$ is given by Mattig (1959) as

$$N(m) = \frac{4\pi n A^3}{3QH_0^3} \{\tfrac{1}{2}[1 + A + \sqrt{(1+2A)}]\}^{-3}. \tag{32}$$

The equation for $N(m)$ for the steady-state model has been given in parametric form by Bondi and Gold (1948) as

$$N(m) = \text{const.} \left[\ln(1+z) - \frac{z(2+3z)}{2(1+z)^2}\right], \tag{33}$$

which, together with the $[m, z]$ relation from equation (23), permits us to tabulate $N(m)$.

Several steps are now required to put equations (30), (32), and (33) into useful form for comparison with the observations. (1) Because the $k_R$ correction is very small for red shifts less than $\frac{1}{2}$, any counts made in the future will undoubtedly be confined to the red spectral region λλ 6200–7500 A. Therefore, we compute $N(m)$ for the $m_R$ magnitude system already discussed. (2) Field galaxies rather than clusters of galaxies will be used for any future counts, which means that the constant term in equations (23′), (24′), and (25′) will not be 20.266 because the mean absolute magnitude of the field galaxies is

fainter than that of the brightest cluster members. The value of $C$ for field galaxies observed in the $m_R$ wave-length band pass is computed as follows.

Galaxies in the general field are a mixture of types. From a sample of 768 galaxies in the Shapley-Ames Catalogue brighter than catalogue magnitude 13.0, and north of $\delta = -30°$, the galaxy types are distributed according to Table 2, which is from an unpublished study by the writer. The sample includes members of the Virgo Cluster.

The average color index of this sample of galaxies can be computed by (1) noting that the absolute magnitude $M_p$ of galaxies selected by apparent magnitude is not a function of galaxy type (see HMS 1956, Table CI) and (2) by adopting the mean colors for the various types given in Table 2. Adding the total intensity of the sample in $m_p$ and $m_v$ wave lengths, weighted by the combined percentages in Table 2 gives $\langle m_p - m_v \rangle = 0.731$. We take this to be representative of galaxies in the general field in a sample chosen according to apparent magnitude. The mean $m_P - m_R$ index will be approximately $1.5\ (0.731) \cong 1.10$.

TABLE 2

DISTRIBUTION OF TYPES FOR GALAXIES IN GENERAL FIELD

| Type | No | Per Cent Total | $m_p - m_v$ | Type | No | Per Cent Total | $m_p - m_v$ |
|---|---|---|---|---|---|---|---|
| E. | 113 | 14 71 | 0 90 | SB0 | 30 | 3 91 | 0 90 |
| S0 | 74 | 9 64 | 90 | SBa | 27 | 3 52 | 80 |
| Sa | 66 | 8 59 | 80 | SBb | 48 | 6 25 | 75 |
| Sb | 115 | 14 97 | 75 | SBc | 15 | 1 95 | 55 |
| Sc | 258 | 33 59 | 0 55 | Irr. | 22 | 2 86 | 0 55 |

Table CI of HMS (1956) shows that the difference in absolute magnitude between the first-ranked cluster galaxy and the mean of the field galaxies in the red-shift catalogue is $\Delta m_p = 2^m.04$. Therefore, equation (26) becomes

$$m_p - k_p = 5 \log z + 23.616 \qquad (z \ll 1) \quad (34)$$

for the average field galaxy, and, because $m_P - m_R \cong 1.10$,

$$m_R - k_R = 5 \log z + 22.516 \qquad (z \ll 1) \quad (35)$$

Therefore, the constant $C$ in equations (23), (24), and (25) has the value 22.516 for the average field galaxy in the red-shift catalogue observed on a red magnitude system.[1] Consequently, the parameter $A$ in equation (29) has the value

$$\log A = 0.2\,(m_R - k_R - 22.516)\,. \qquad (29')$$

The final step to compare equations (30), (32), and (33) with the actual counts is to determine the lumped value of the constants by requiring that

$$\log N(m) = 0.6 m_p - 8.87 \quad (36)$$

for $z \ll 1$ (at bright magnitudes) as given by Holmberg (1957) from his corrections to the magnitude system of the Shapley-Ames Catalogue. Transforming equation (36) to the $m_R$ system by $m_P - m_R = 1.10$ gives, for $z \ll 1$,

[1] This computation is somewhat schematic because the field galaxies listed in the red-shift catalogue are undoubtedly biased toward bright absolute magnitudes. Consequently, $\Delta m_p$ will actually exceed 2.04 mag. by an unknown amount, and $C$ will be somewhat larger than 22.516. This will not, however, affect the conclusion of this section.

$$\log N(m) = 0.6 m_R - 8.21 , \tag{37}$$

which we require to be given by equations (30), (32), and (33) for bright magnitudes.

The system of equations (29′), (31), (30), (32), and (33), used in that order, can now be used to compute $N(m)$ for various $q_0$ values. However, series expansions are required of equations (30) and (33) until $P$ and $z$ become large enough that the available tables of $\sin^{-1} P$ and $\ln(1+z)$ can be used. The series expansions of equations (30) for small $P$ are

$$[P\sqrt{(1+P^2)} - \text{arc sinh } P] \equiv \tfrac{2}{3}P^3 - \tfrac{1}{5}P^5 + \tfrac{12}{112}P^7 + \ldots ,$$
$$[\text{arc sin } P - P\sqrt{(1-P^2)}\,] \equiv \tfrac{2}{3}P^3 + \tfrac{1}{5}P^5 + \tfrac{12}{112}P^7 + \ldots . \tag{38}$$

The series expansion of equation (33) for the steady-state case is

$$\left[\ln(1+z) - \frac{z(2+3z)}{2(1+z)^2}\right] \equiv \tfrac{1}{3}z^3 - \tfrac{3}{4}z^4 + \tfrac{6}{5}z^5 - \tfrac{5}{3}z^6 + \tfrac{15}{7}z^7 - \tfrac{21}{8}z^8 + \ldots . \tag{39}$$

The results of the computations are given in Table 3 for $m_R - k_R$ values ranging from eighth to fortieth magnitude. The steady-state model ($q_0 = -1$) is compared with seven exploding models with $q_0 = 0$, $\frac{1}{2}$, 1, $2\frac{1}{2}$, 5, $8\frac{1}{2}$, and 13. These particular evolving models represent a hyperbolic universe of zero density ($q_0 = 0$), Euclidean space ($q_0 = \frac{1}{2}$) of density $\rho_0 = 3H_0^2/8\pi G$, and closed oscillating universes whose radii of curvature are $R_0 = c/H_0 n_i$, where $n_i = 1, 2, 3, 4$, and 5 for $q_0 = 1$, $2\frac{1}{2}$, 5, $8\frac{1}{2}$, and 13 (see eq. [10′]). The results for the evolving models are shown graphically in Figure 3.

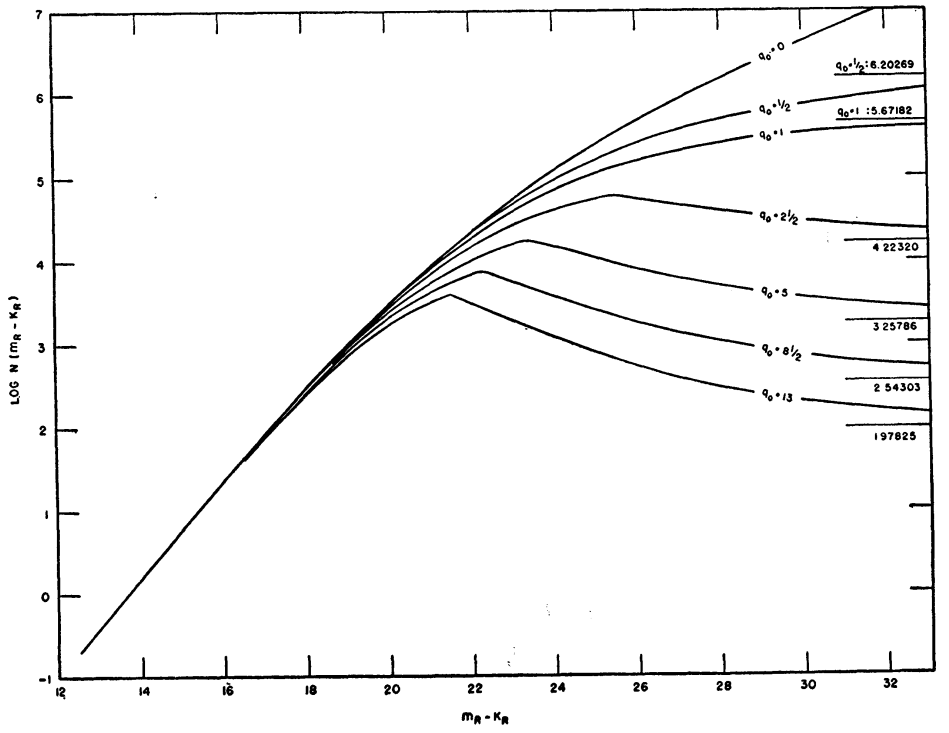


FIG. 3.—The count-magnitude relation for various $q_0$ values. Magnitudes are on the red system. The curves refer to field galaxies. Correction for the periodicity of eq. (30) has not been made. The antipodal point is reached where the curves have a maximum.

TABLE 3*

PREDICTED GALAXY COUNT-MAGNITUDE RELATION FOR FIELD GALAXIES

| $m_R - k_R$ | $q_o = -1$ | $q_o = 0$ | $q_o = 0.5$ | $q_o = 1$ | $q_o = 2.5$ | $q_o = 5$ | $q_o = 8.5$ | $q_o = 13$ |
|---|---|---|---|---|---|---|---|---|
| 8.0 | −3.4116 | −3.4116 | −3.4116 | −3.4116 | −3.4116 | −3.4116 | −3.4116 | −3.4116 |
| 8.5 | −3.1124 | −3.1120 | −3.1120 | −3.1120 | −3.1120 | −3.1120 | −3.1120 | −3.1120 |
| 9.0 | −2.8133 | −2.8126 | −2.8126 | −2.8126 | −2.8126 | −2.8126 | −2.8126 | −2.8126 |
| 9.5 | −2.5144 | −2.5132 | −2.5132 | −2.5132 | −2.5132 | −2.5132 | −2.5132 | −2.5133 |
| 10.0 | −2.2159 | −2.2141 | −2.2141 | −2.2141 | −2.2141 | −2.2141 | −2.2141 | −2.2141 |
| 10.5 | −1.9177 | −1.9151 | −1.9151 | −1.9151 | −1.9151 | −1.9151 | −1.9152 | −1.9152 |
| 11.0 | −1.6200 | −1.6164 | −1.6165 | −1.6165 | −1.6165 | −1.6165 | −1.6165 | −1.6166 |
| 11.5 | −1.3229 | −1.3181 | −1.3181 | −1.3181 | −1.3181 | −1.3182 | −1.3182 | −1.3183 |
| 12.0 | −1.0265 | −1.0202 | −1.0202 | −1.0202 | −1.0202 | −1.0203 | −1.0204 | −1.0205 |
| 12.5 | −0.7311 | −0.7228 | −0.7228 | −0.7228 | −0.7229 | −0.7230 | −0.7231 | −0.7233 |
| 13.0 | −0.4368 | −0.4261 | −0.4261 | −0.4262 | −0.4262 | −0.4264 | −0.4266 | −0.4269 |
| 13.5 | −0.1438 | −0.1302 | −0.1303 | −0.1303 | −0.1304 | −0.1307 | −0.1310 | −0.1314 |
| 14.0 | +0.1473 | +0.1646 | +0.1646 | +0.1645 | +0.1643 | +0.1639 | +0.1634 | +0.1627 |
| 14.5 | 0.4364 | 0.4582 | 0.4581 | 0.4580 | 0.4576 | 0.4571 | 0.4563 | 0.4552 |
| 15.0 | 0.7228 | 0.7502 | 0.7500 | 0.7499 | 0.7493 | 0.7484 | 0.7472 | 0.7455 |
| 15.5 | 1.0060 | 1.0403 | 1.0400 | 1.0397 | 1.0388 | 1.0374 | 1.0355 | 1.0330 |
| 16.0 | 1.2854 | 1.3279 | 1.3275 | 1.3270 | 1.3258 | 1.3235 | 1.3206 | 1.3167 |
| 16.5 | 1.5601 | 1.6127 | 1.6120 | 1.6113 | 1.6093 | 1.6059 | 1.6013 | 1.5952 |
| 17.0 | 1.8295 | 1.8939 | 1.8929 | 1.8918 | 1.8887 | 1.8835 | 1.8763 | 1.8672 |
| 17.5 | 2.0925 | 2.1710 | 2.1694 | 2.1678 | 2.1630 | 2.1551 | 2.1442 | 2.1304 |
| 18.0 | 2.3482 | 2.4430 | 2.4406 | 2.4382 | 2.4310 | 2.4191 | 2.4028 | 2.3823 |
| 18.5 | 2.5956 | 2.7094 | 2.7057 | 2.7020 | 2.6912 | 2.6736 | 2.6496 | 2.6198 |
| 19.0 | 2.8337 | 2.9690 | 2.9636 | 2.9582 | 2.9422 | 2.9164 | 2.8816 | 2.8393 |
| 19.5 | 3.0620 | 3.2211 | 3.2131 | 3.2052 | 3.1820 | 3.1449 | 3.0959 | 3.0373 |
| 20.0 | 3.2795 | 2.4649 | 3.4533 | 3.4419 | 3.4087 | 3.3566 | 3.2893 | 3.2110 |
| 20.5 | 3.4856 | 3.6996 | 3.6831 | 3.6669 | 3.6204 | 3.5490 | 3.4594 | 3.3584 |
| 21.0 | 3.6801 | 3.9246 | 3.9014 | 3.8789 | 3.8153 | 3.7201 | 3.6048 | 3.4795 |
| 21.5 | 3.8627 | 4.1397 | 4.1076 | 4.0769 | 3.9918 | 3.8688 | 3.7256 | 3.5742 |
| 22.0 | 4.0336 | 4.3445 | 4.3010 | 4.2600 | 4.1491 | 3.9951 | 3.8232 | 3.4841 |
| 22.5 | 4.1929 | 4.5392 | 4.4813 | 4.4276 | 4.2868 | 4.0998 | 3.8282 | 3.3862 |
| 23.0 | 4.3411 | 4.7239 | 4.6483 | 4.5797 | 4.4070 | 4.1851 | 3.7456 | 3.2840 |
| 24.0 | 4.6062 | 5.0657 | 4.9431 | 4.8379 | 4.5910 | 4.1614 | 3.5721 | 3.0790 |
| 25.0 | 4.8336 | 5.3748 | 5.1885 | 5.0398 | 4.7190 | 4.0273 | 3.4030 | 2.8879 |
| 26.0 | 5.0285 | 5.6570 | 5.3899 | 5.1940 | 4.7287 | 3.8993 | 3.2501 | 2.7201 |
| 27.0 | 5.1958 | 5.9178 | 5.5533 | 5.3100 | 4.6477 | 3.7852 | 3.1180 | 2.5781 |
| 28.0 | 5.3401 | 6.1623 | 5.6849 | 5.3967 | 4.5744 | 3.6869 | 3.0072 | 2.4605 |
| 29.0 | 5.4652 | 6.3945 | 5.7904 | 5.4616 | 4.5106 | 3.6046 | 2.9159 | 2.3645 |
| 30.0 | 5.5742 | 6.6176 | 5.8747 | 5.5102 | 4.4566 | 3.5367 | 2.8416 | 2.2869 |
| 31.0 | 5.6699 | 6.8340 | 5.9419 | 5.5470 | 4.4117 | 3.4814 | 2.7816 | 2.2244 |
| 32.0 | 5.7544 | 7.0455 | 5.9954 | 5.5749 | 4.3749 | 3.4366 | 2.7333 | 2.1744 |
| 33.0 | 5.8295 | 7.2536 | 6.0380 | 5.5963 | 4.3448 | 3.4006 | 2.6947 | 2.1344 |
| 34.0 | 5.8967 | 7.4593 | 6.0718 | 5.6127 | 4.3205 | 3.3716 | 2.6638 | 2.1025 |
| 35.0 | 5.9572 | 7.6632 | 6.0987 | 5.6254 | 4.3009 | 3.3485 | 2.6391 | 2.0770 |
| 36.0 | 6.0119 | 7.8658 | 6.1201 | 5.6353 | 4.2852 | 3.3300 | 2.6195 | 2.0568 |
| 37.0 | 6.0617 | 8.0677 | 6.1371 | 5.6431 | 4.2726 | 3.3153 | 2.6032 | 2.0407 |
| 38.0 | 6.1073 | 8.2689 | 6.1506 | 5.6491 | 4.2626 | 3.3035 | 2.5913 | 2.0279 |
| 39.0 | 6.1492 | 8.4698 | 6.1613 | 5.6539 | 4.2545 | 3.2942 | 2.5814 | 2.0177 |
| 40.0 | 6.1879 | 8.6703 | 6.1698 | 5.6576 | 4.2481 | 3.2867 | 2.5735 | 2.0096 |
| limit | ∞ | ∞ | 6.2027 | 5.6718 | 4.2232 | 3.2579 | 2.5430 | 1.9782 |

*Tabulated is log N(m)

Curiously, a maximum occurs in $N(m)$ for those models with $q_0 \geq 1$. Recall that $N(m)$ is defined as the number of galaxies per square degree *brighter* than apparent magnitude $m$. Consequently, passage of $N(m)$ through a maximum and a subsequent decline is impossible because the *total* number of sources can never be made smaller by going to fainter magnitudes. The behavior is explained by the periodicity of the relevant equations. The opposite pole of the universe is reached at the magnitude where $N(m)$ is a maximum, and the distance vector $u$ is beginning its journey back toward the observer, but pointed in the opposite direction from which it began.

The situation is clear by analogy with the surface of a sphere of radius $R$. When the distance $r$ along the surface has a value $\pi R$, the complete area of the sphere has been covered once. The equation for the area of the spherical cap encompassed within the distance $r$ is

$$S(r) = 2\pi R^2 \left(1 - \cos \frac{r}{R}\right) \qquad (r \leq \pi R) . \quad (40)$$

When $r > \pi R$, the area given formally by equation (40) begins to decrease from its maximum value of $4\pi R^2$. Thought shows that the total area counted from $r = 0$ to $r > \pi R$ is $8\pi R^2 - 2\pi R^2 (1 - \cos r/R) \equiv 2\, S(\max) - S(r)$. The periodicity of equation (40) is taken into account by this procedure. The periodicity of equation (30) may be treated in the same way for distances larger (magnitudes fainter) than the maxima of Figure 3, i.e., for distances beyond the antipodal point when the "universe has been counted once." Consequently, for those curves where $q_0 > 1$, the correct number count, $N_c(m)$, is given by

$$N_c(m) = 2N(\text{max.}) - N(m), \qquad \text{for } m > m(\text{max.}), \quad (41)$$

where $N(m)$ is the number calculated formally by equation (30). The $N_c(m)$ values computed from equation (41) are tabulated in Table 4. It is important to note that the $N_c(m)$ values rather than $N(m)$ are the numbers which will actually be observed at the telescope. The resulting relation between $N_c(m)$ and $m$ is shown in Figure 4. For later comparison, the lines of constant red shift are drawn as computed from equations (24) and (25) with $C = 22.516$. Note that the red shifts become extremely large for faint magnitudes. The asymptotic behavior of log $N(m)$ and log $N_c(m)$ is discussed in Appendix A, where the explicit equations are given.

Returning for the moment to Figure 3, we ask for the magnitude at which $N(m)$ has a maximum. As mentioned before, the antipole of the universe is reached at this point. For $N(m)$ to have a maximum, $P$ must have a maximum and $dP/dA = 0$. Differentiation of equation (31) shows that $N(m)$ has a maximum when

$$A = \frac{(2q_0 - 1) + q_0\sqrt{(2q_0 - 1)}}{(q_0 - 1)^2} . \quad (42)$$

The $m_R - k_R$ values required for maximum $N(m)$ were computed from equations (42) and (29′) and are given in Table 5, together with values of log $N(m)_{\max}$ and $1 + z$ (computed from eq. [28]). From Figure 3 it is evident that the antipole is not reached for models with $\frac{1}{2} < q_0 < 1$, even though the universe is closed. Furthermore, the fact that that $N_c(m)$ approaches an asymptotic limit for each model studied with $q_0 > 0$ means that we have reached, in each case, an observational horizon beyond which no information crosses.

We now have the necessary information to assess the ability of the 200-inch telescope to discriminate between world models using galaxy counts. To obtain $N_c(m)$ in terms of the observed magnitude $m_R$, we must correct Figure 4 for the $k_R$ term by shifting the abscissa value of each line of constant $z$ by an amount $k_R$ magnitudes, keeping the ordi-

nate constant. Since lines of constant $z$ are also lines of constant $k_R$, the shifts are easily made if $k_R = f(z)$ is known. This procedure gives the theoretical diagram plotted in terms of observables only. In the absence of precise $k_R$ values, we can make the correction only approximately, but the error in this approximation is undoubtedly less than 0.2 mag., which is negligible for the conclusions concerning the feasibility of galaxy counts to test the models.

Figure 5 shows the relevant part of Figure 4 corrected by assuming

$$k_R = 2z - 0.6 \qquad \text{for } 0.3 < z \leq 1 , \quad (43)$$

which was obtained from preliminary calculations using the M32 $I(\lambda)$-curve (see HMS, Appendix B). As mentioned in the last section, more accurate values of $k_R$ in the range

TABLE 4

COUNT-MAGNITUDE RELATION FOR FIELD GALAXIES CORRECTED FOR PERIODICITY OF EQUATION (30)*

| $m_R - k_R$ | $q_0$ | | | |
|---|---|---|---|---|
| | 2 5 | 5 | 8 5 | 13 |
| 21 5 | | | | 3 5756 |
| 22 0 | | | . . . | 3 6500 |
| 22 5 | | | 3 9001 | 3 7060 |
| 23 0 | | . . . . | 3 9596 | 3 7476 |
| 24 0 | | 4 3073 | 4 0392 | 3 8004 |
| 25 0 | . . . | 4 3828 | 4 0845 | 3 8288 |
| 26 0 | 4 8054 | 4 4291 | 4 1106 | 3 8445 |
| 27 0 | 4 8633 | 4 4578 | 4 1260 | 3 8535 |
| 28 0 | 4 9025 | 4 4761 | 4 1355 | 3 8589 |
| 29 0 | 4 9295 | 4 4881 | 4 1416 | 3 8623 |
| 30 0 | 4 9485 | 4 4962 | 4 1456 | 3 8646 |
| 31 0 | 4 9620 | 4 5019 | 4 1484 | 3 8661 |
| 32 0 | 4 9718 | 4 5059 | 4 1504 | 3 8672 |
| 33 0 | 4 9791 | 4 5089 | 4 1518 | 3 8680 |
| 34 0 | 4 9846 | 4 5111 | 4 1528 | 3 8686 |
| 35 0 | 4 9887 | 4 5127 | 4 1536 | 3 8690 |
| 36 0 | 4 9918 | 4 5139 | 4 1539 | 3 8693 |
| 37 0 | 4 9943 | 4 5149 | 4 1546 | 3 8695 |
| 38 0 | 4 9962 | 4 5156 | 4 1550 | 3 8697 |
| 39 0 | 4 9976 | 4 5162 | 4 1552 | 3 8699 |
| 40 0 | 4 9988 | 4 5166 | 4 1554 | 3 8700 |
| limit | 5 0031 | 4 5183 | 4 1562 | 3 8704 |

* Tabulated is log $N_c(m)$ All entries not tabulated are the same as in Table 3

$0 < z < 1.0$ will be available when the true $I(\lambda)$-curves for galaxies are available from work now in progress by J. B. Oke.

Figure 5 shows that the difference in log $N(m_R)$ between the extremes of the models becomes large beyond $m_R = 20$. However, it will be recalled that $q_0$ lies between $+3$ and $-1$, with the most probable limits being 0 and $+2$. Very small difference exists in $N(m)$ between the closed model with $q_0 = +1$ and the open, "empty" model $q_0 = 0$. The predicted difference is $\Delta \log N(m) = 0.12$ at $m_R = 22$ (see Fig. 5), a difference which would certainly be buried in the probable errors of any observational data. The $\Delta \log N(m) = 0.12$, read as a magnitude difference, amounts to only $\Delta m_R = 0^m.28$ at $m_R = 22$. Hence an observational error of this amount would change the conclusion from the open, empty model with $q_0 = 0$, to a closed, oscillating model with $q_0 = +1$. The extreme difficulty

of determining the magnitudes of galaxies is well known, and systematic errors due to the aperture effect (HMS 1956, Appendix A) can easily reach 0.28 mag., thus masking any choice. A similar situation holds for galaxy counts on the steady-state theory. Figure 6 compares the log $N(m_R - k_R)$ curves for $q_0 = 0$, $q_0 = 2\frac{1}{2}$, and for the steady-state model. As before, the differences between the models are so small that no practical test is possible. Therefore, the analysis of the count data by Bondi and Gold (1948) and later by Bondi (1952), which purports to show that the steady-state predictions are closer to the actual counts than the predictions of the exploding models, appears to have no weight whatsoever.

It would therefore seem impossible to find the correct world model from galaxy counts, and any attempt to do so appears to be a waste of telescope time. This is particularly true because the calculations leading to Figures 5 and 6 are idealized and the true relations are expected to be less definite. For example, it is well known that galaxies are not homogeneously distributed on the plane of the sky but show a strong tendency to cluster.

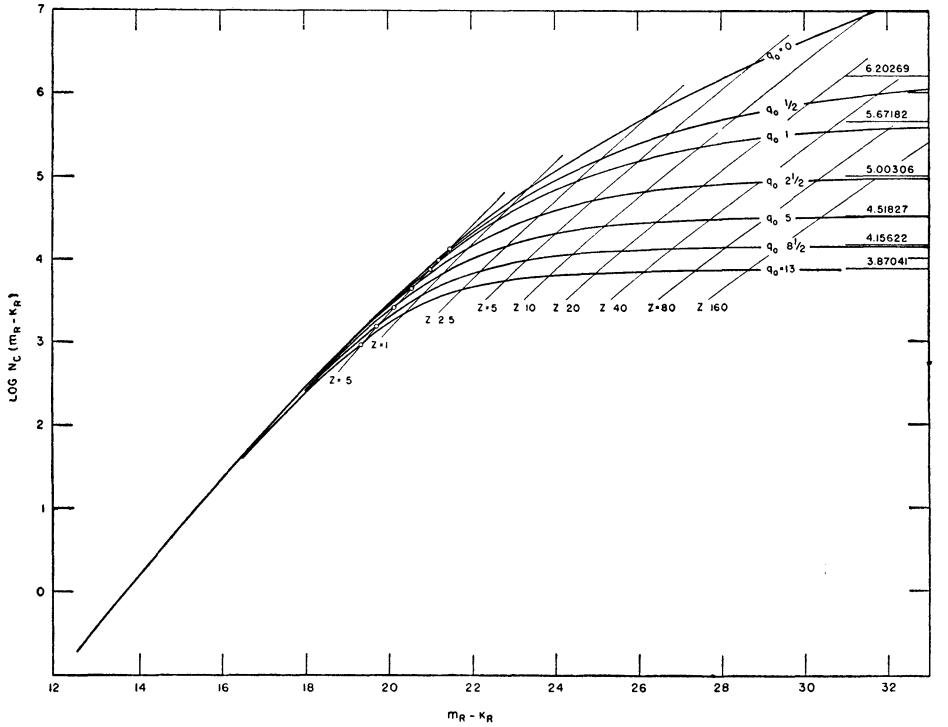


FIG. 4.—Same as Fig 3 except that the curves have been corrected for the periodicity of eq. (30). The asymptotic values of log $N_c(m)$ are given on the right. Lines of constant red shift are shown

TABLE 5

PARAMETERS OF ANTIPOLE OF UNIVERSE

| $q_0$ | log $N(m)_{max}$ | $m_R - k_R$ | $1+z$ |
|---|---|---|---|
| $2\frac{1}{2}$ | 4 76873 | 25 526 | 8 000 |
| 5. | 4 24046 | 23 396 | 4 500 |
| $8\frac{1}{2}$ | 3 86564 | 22 260 | 3 556 |
| 13 | 3 57491 | 21 495 | 3 125 |

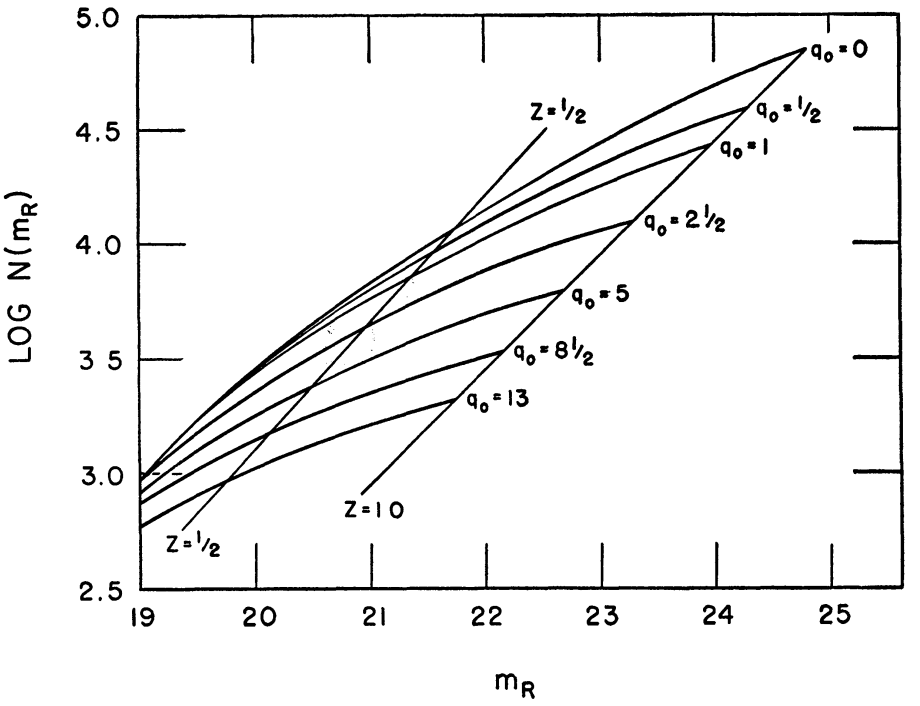


FIG 5.—Same as Fig 4 but with the $k_R$ correction applied to the magnitudes This diagram shows what will actually be observed at the telescope The lines of constant red shift for $z = 0\ 5$ and $z = 1\ 0$ are shown. Note the very small difference between $q_0 = 1$ and $q_0 = 0$ in the log $N(m)$ values at $m_R = 22\ 0$

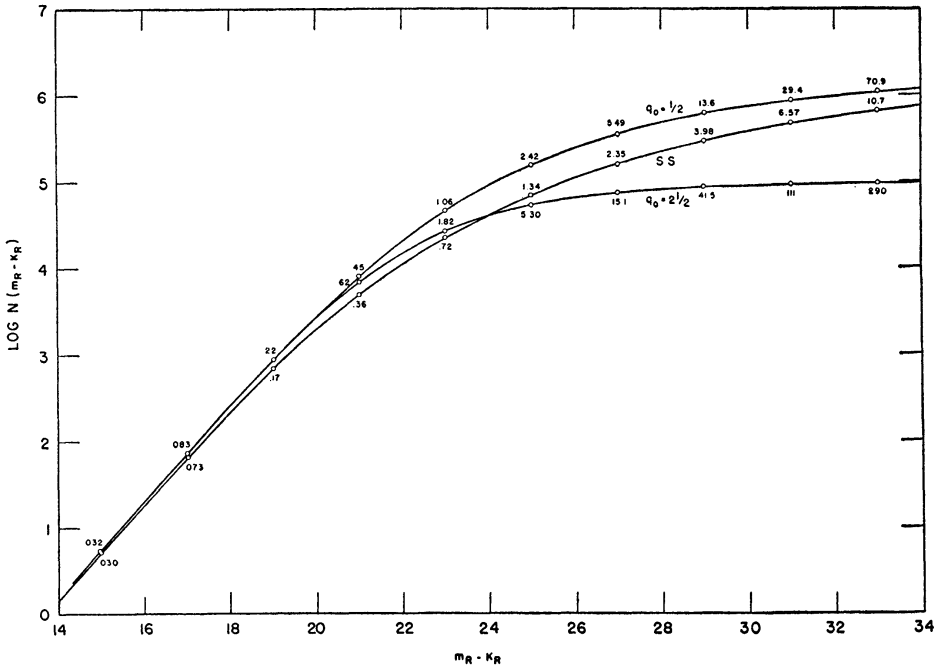


FIG. 6 —Comparison of the count-magnitude relation for the steady-state model ($q_0 = -1$) and the two exploding models $q_0 = \frac{1}{2}$ and $q_0 = 2\frac{1}{2}$ Note the extremely small difference in the predicted log $N(m)$ values between the three models for magnitudes brighter than $m_R - k_R = 23$. Values of the red shift $z$ are shown on each curve.

Even if they are homogeneously distributed on a very large scale, the fluctuations in any sample area chosen for counting preclude with certainty attempts to use counts for deciding between models. Furthermore, no account has been taken of the spread in the absolute luminosity of galaxies or of the evolutionary effect of a change in $L(\lambda)$ as a function of time. Finally, as previously mentioned, the absolute magnitude of the average field galaxy is undoubtedly fainter than has been assumed in fixing the constant $C$ at 22.516 because of the magnitude bias of the red-shift catalogue. Therefore, the curves of Figures 3, 4, 5, and 6 should be shifted to even fainter magnitudes than shown, and the differences at, say, $m_R = 22$ will become even smaller.

## IV. ANGULAR DIAMETERS

### *a) Diameters of Rigid Rods (Metric Diameters)*

To obtain equations for the angular diameter of objects in an expanding universe, we must know the metric distance of the source. This is given by the standard analysis of the line element as follows. The line element is given by equation (1), or more explicitly by

$$ds^2 = c^2 dt^2 - R^2(t)\left[\frac{dr^2}{1-kr^2} + r^2(d\theta^2 + \sin^2\theta d\phi^2)\right], \tag{44}$$

where $r$, $\theta$, and $\phi$ are dimensionless, co-moving co-ordinates. The equation for a light-track is the null geodesic $ds^2 = 0$. In terms of the dimensionless parameter distance $u$ of equations (1) and (16), the connection between the time of emission $t_1$, the time of reception of the photons, $t_0$, and the dimensionless radial co-ordinate $r$ is given by

$$u = c\int_{t_1}^{t_0} \frac{dt}{R(t)} = \int_0^{r_1} \frac{dr}{\sqrt{(1-kr^2)}} \tag{45}$$

where the observer is taken to be at $r = 0$. The right side of equation (45) integrates to

$$u = \begin{cases} \sin^{-1} r_1 & k = +1 \\ r_1 \quad \text{for} & k = 0 \\ \sinh^{-1} r_1 & k = -1\,, \end{cases} \tag{46}$$

or

$$r_1 = \begin{cases} \sin u & k = +1 \\ u \quad \text{for} & k = 0 \\ \sinh u & k = -1\,. \end{cases} \tag{47}$$

The metric distance at the time of photon emission is $r_1 R_1$, which by equation (47) is equal to $R_1\,\sigma(u)$, where $\sigma(u) \equiv \sin u$, $u$, or $\sinh u$ for $k = 1, 0$, or $-1$. This is the $\sigma(u)$ which occurs in equation (17).

A source whose metric distance is $R_1\,\sigma(u)$ at the time of photon emission and whose linear diameter is $y$ has an observed angular diameter at $t_0$ of

$$\theta_0 = \frac{y}{R_1\sigma(u)}\,. \tag{48}$$

Substitution of $R_1 = R_0/(1+z)$ from equation (18) gives

$$\theta_0 = \frac{y(1+z)}{R_0\sigma(u)}\,, \tag{49}$$

which can be put in terms of the observables $z$ and $m$, or $m$ alone from Mattig's analysis (1958) used in Section II. Mattig shows that

$$r_1 \equiv \sigma(u) = \frac{c}{R_0 H_0 q_0^2 (1+z)} \{ q_0 z + (q_0 - 1)[\sqrt{(1+2q_0 z)}] \} \quad (50)$$

for all $q_0 \geq 0$, which, when substituted in equation (49) and simplified by equations (24) and (29), gives

$$\theta_0 = \frac{\text{const.}\,(1+z)^2}{A} \qquad \text{for all } q_0 \geq 0\,, \quad (51)$$

which is the required result for evolving models.

The equation for the steady-state model follows immediately from equations (49) and (21) of Section II, where it was shown that $R_0\,\sigma(u) \equiv R_0 u = cz/H_0$. Substitution of equation (21) in equation (49) gives

$$\theta_0 = \text{const.}\left(\frac{1+z}{z}\right) \qquad \text{for } q_0 = -1\,, \quad (52)$$

which reduces to equation (51) by equations (23) and (29). Therefore, equation (51) gives the angle subtended by a standard rod at various distances characterized by a redshift value $z$ for all models considered here. These angles will be called "metric diameters" to distinguish them from isophotal diameters.

To minimize the effect of the intrinsic dispersion of the linear diameters $y$, any future observations will undoubtedly be made of the characteristic size of clusters of galaxies rather than of individual galaxies. Consequently, the value of $C$ in equation (29) is taken as 20.266, since this corresponds to the brightest galaxy of a cluster rather than to the average of the field galaxies.

The results of the computations are given in Table 6, where either $m_R - k_r$ or $z$ can be considered as the argument. If $z$ is taken as argument, the $z = f(m_R - k_R)$ of Table 1 must be used. The results are shown in Figure 7 with $m_R - k_R$ as abscissa. Notice that the metric angular diameter for all evolving models ($q_0 \geq 0$) has a minimum value at a definite magnitude and begins to increase again for fainter magnitudes. For the steady-state model, $\theta_0$ decreases asymptotically to the value of the constant in equation (52) as $z \to \infty$. This behavior was first pointed out by Hoyle (1959), who proposes the presence or absence of a minimum as a test between the models. The test is important because it uses only the presence or absence of an observable effect rather than a measured quantity. It is important to note, however, that the minimum occurs beyond the optical limit of the 200-inch telescope (see Fig. 7), and such a test is therefore in the domain of radio astronomy. *Note also the test refers to metric diameters and not isophotal diameters.*

Returning to the optical problem, we ask whether the predicted differences shown in Figure 7 are large enough in the range of the 200-inch to constitute a test for $q_0$. For an answer, the curves of Figure 7 must be corrected for the $k_R$ term by shifting the curves along the abscissa an amount $k_R = f(z)$ given provisionally by equation (43). To facilitate the correction, lines of constant $z$ are shown as computed from equations (28) and (29). The resulting diagram, corrected to $z = +1$, is shown in Figure 8, with the directly observed magnitude $m_R$ plotted as abscissa. The plate limit for cluster counts is probably $m_R \cong 21$. Here the difference in log $\theta_0$ between the steady-state model ($q_0 = -1$) and $q_0 = +1$ is only 0.195; or $\theta_{0,1}/\theta_{0,-1} = 1.57$, assuming a constant linear diameter $y$. The limit $m_R = 21$ is perhaps fainter than the 200-inch can actually observe because this magnitude is on the system of the first-ranked galaxy in a cluster and we must be able to count a large number of the fainter cluster members to determine the cluster size. The cluster must be sampled to perhaps $m_R = 23$ or $m_R = 24$, which is beyond the plate limit.

## TABLE 6

### METRIC ANGULAR DIAMETERS ON THE MAGNITUDE SYSTEM OF THE FIRST RANKED CLUSTER GALAXY* †

| $m_R = k_R$ | $q_0 = -1$ | $q_0 = 0$ | $q_0 = 0.5$ | $q_0 = 1$ | $q_0 = 2.5$ | $q_0 = 5$ | $q_0 = 8.5$ | $q_0 = 13$ |
|---|---|---|---|---|---|---|---|---|
| 8.0 | 285.92 | 285.92 | 285.92 | 285.93 | 285.93 | 285.94 | 285.95 | 285.97 |
| 8.5 | 227.52 | 227.53 | 227.53 | 227.53 | 227.54 | 227.55 | 227.56 | 227.58 |
| 9.0 | 181.14 | 181.14 | 181.15 | 181.15 | 181.16 | 181.17 | 181.19 | 181.22 |
| 9.5 | 144.29 | 144.30 | 144.30 | 144.30 | 144.32 | 144.33 | 144.36 | 144.39 |
| 10.0 | 115.02 | 115.03 | 115.04 | 115.04 | 115.05 | 115.08 | 115.11 | 115.15 |
| 10.5 | 91.77 | 91.78 | 91.79 | 91.79 | 91.81 | 91.84 | 91.88 | 91.93 |
| 11.0 | 73.30 | 73.32 | 73.32 | 73.33 | 73.35 | 73.39 | 73.44 | 73.50 |
| 11.5 | 58.63 | 58.65 | 58.66 | 58.67 | 58.69 | 58.74 | 58.80 | 58.88 |
| 12.0 | 46.98 | 47.00 | 47.01 | 47.02 | 47.05 | 47.11 | 47.19 | 47.29 |
| 12.5 | 37.72 | 37.74 | 37.76 | 37.77 | 37.81 | 37.88 | 37.93 | 38.11 |
| 13.0 | 30.36 | 30.39 | 30.41 | 30.43 | 30.48 | 30.57 | 30.69 | 30.85 |
| 13.5 | 24.51 | 24.55 | 24.57 | 24.60 | 24.66 | 24.77 | 24.93 | 25.13 |
| 14.0 | 19.86 | 19.91 | 19.94 | 19.97 | 20.05 | 20.19 | 20.39 | 20.65 |
| 14.5 | 16.17 | 16.23 | 16.26 | 16.30 | 16.41 | 16.58 | 16.83 | 17.16 |
| 15.0 | 13.23 | 13.30 | 13.35 | 13.39 | 13.53 | 13.75 | 14.06 | 14.48 |
| 15.5 | 10.89 | 10.98 | 11.03 | 11.09 | 11.26 | 11.43 | 11.94 | 12.47 |
| 16.0 | 9.02 | 9.13 | 9.20 | 9.27 | 9.48 | 9.84 | 10.36 | 11.04 |
| 16.5 | 7.53 | 7.66 | 7.75 | 7.84 | 8.11 | 8.57 | 9.23 | 10.12 |
| 17.0 | 6.34 | 6.50 | 6.61 | 6.72 | 7.06 | 7.65 | 8.51 | 9.68 |
| 17.5 | 5.39 | 5.57 | 5.71 | 5.85 | 6.29 | 7.04 | 8.17 | 9.75 |
| 18.0 | 4.62 | 4.84 | 5.01 | 5.19 | 5.74 | 6.72 | 8.23 | 10.38 |
| 18.5 | 4.01 | 4.26 | 4.47 | 4.70 | 5.40 | 6.69 | 8.72 | 11.73 |
| 19.0 | 3.51 | 3.79 | 4.07 | 4.35 | 5.26 | 6.97 | 9.76 | 14.04 |
| 19.5 | 3.10 | 3.42 | 3.77 | 4.13 | 5.30 | 7.59 | 11.49 | 17.67 |
| 20.0 | 2.77 | 3.13 | 3.56 | 4.02 | 5.55 | 8.65 | 14.16 | 23.21 |
| 20.5 | 2.50 | 2.90 | 3.43 | 4.01 | 6.02 | 10.27 | 18.13 | 31.47 |
| 21.0 | 2.27 | 2.71 | 3.38 | 4.12 | 6.76 | 12.63 | 23.91 | 43.64 |
| 21.5 | 2.09 | 2.57 | 3.39 | 4.33 | 7.84 | 15.99 | 32.21 | 61.34 |
| 22.0 | 1.93 | 2.45 | 3.47 | 4.67 | 9.34 | 20.67 | 44.01 | 86.81 |
| 22.5 | 1.80 | 2.36 | 3.62 | 5.16 | 11.38 | 27.15 | 60.59 | 123.02 |
| 23.0 | 1.69 | 2.28 | 3.84 | 5.81 | 14.12 | 36.03 | 83.66 | 173.95 |

*Tabulated is $(1 + z)^2/A$ computed from equations (51) and (52) with const = 1. The constant C in equation (29) for A is 20.266.

†To obtain z as argument use Table 1 for the $m_R - k_R = f(z, q_0)$ relation.

Furthermore, for an actual test to be feasible, the natural dispersion in the linear diameters $y$ must not be so large as to mask the differences shown in Figure 8. That this is so can be determined only by studying bright clusters of galaxies to find the scatter about the straight line part of Figure 8 and checking whether the observational uncertainty is smaller than the predicted differences.

Figure 9 shows log $\theta_0$ ($q_0$) given as a function of $z$ as obtained from Tables 6 and 1. This is a more fundamental plot than Figure 8 because only the ordinate in Figure 9 has intrinsic dispersion while both co-ordinates in Figure 8 have natural variation. Figure 9 shows what can be accomplished observationally. The largest red shift measured to date is $z = 0.46$ (Minkowski 1960) for the cluster centered on radio source 3C 295. The direct plates of this cluster (Eastman 103*a*-E + Schott RG 2) show that the brightest cluster galaxy is within 2 mag. of the plate limit in these wave lengths (λλ 6200–6900 A); consequently, the cluster is close to the limit for which cluster sizes can be determined. Perhaps with great effort clusters with $z \cong 0.60$ can be used, but this appears to be the absolute limit for the determination of geometrical size with the 200-inch telescope. At $z = 0.6$, log $\theta_0(q = +1)$ − log $\theta_0(q = -1) = 0.21$ or $\theta_{0,1}/\theta_{0,-1} = 1.62$. It is problematical whether this difference is large enough to give a significant decision between the models.

A number of clusters with known $z$ values are presently available to make the test. Humason lists 10 clusters with $z$ near 0.2 in his red-shift catalogue (HMS 1956). There

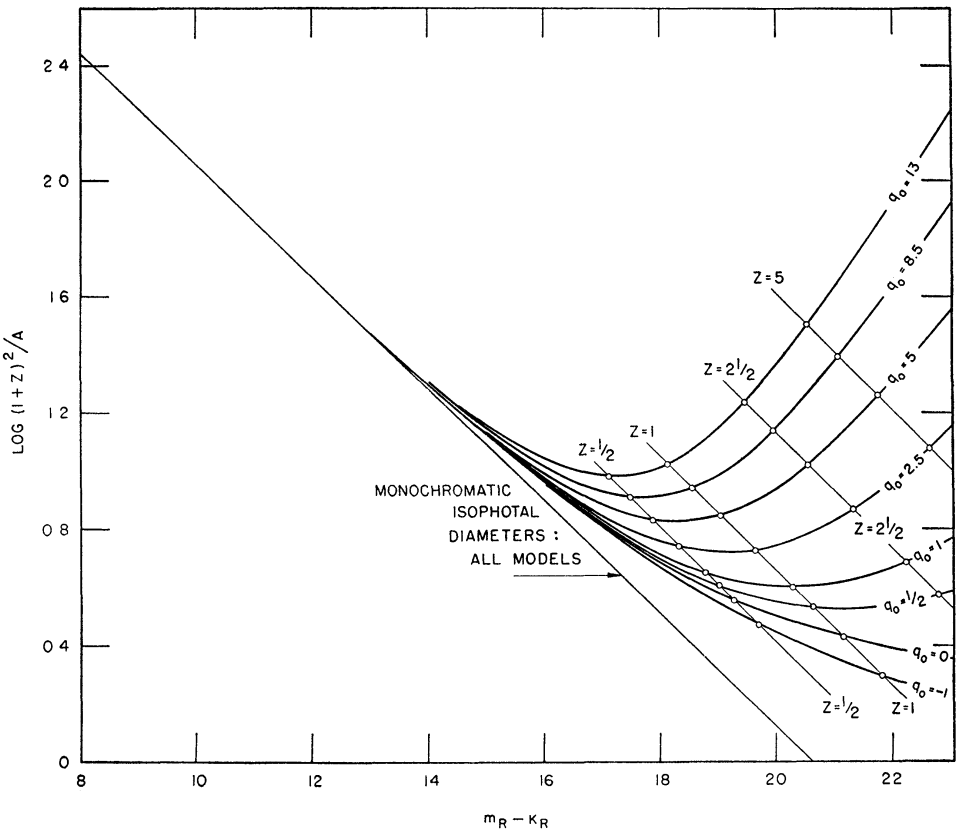


FIG 7.—*Metric* diameters of either individual galaxies or of clusters of galaxies computed on the magnitude system of the brightest cluster galaxy. No normalization of the ordinate to agree with observational data has been made The steady-state model ($q_0 = -1$) and seven exploding models are shown Lines of constant red shift are given. The straight line gives the *isophotal* diameters for all models by eq (56).

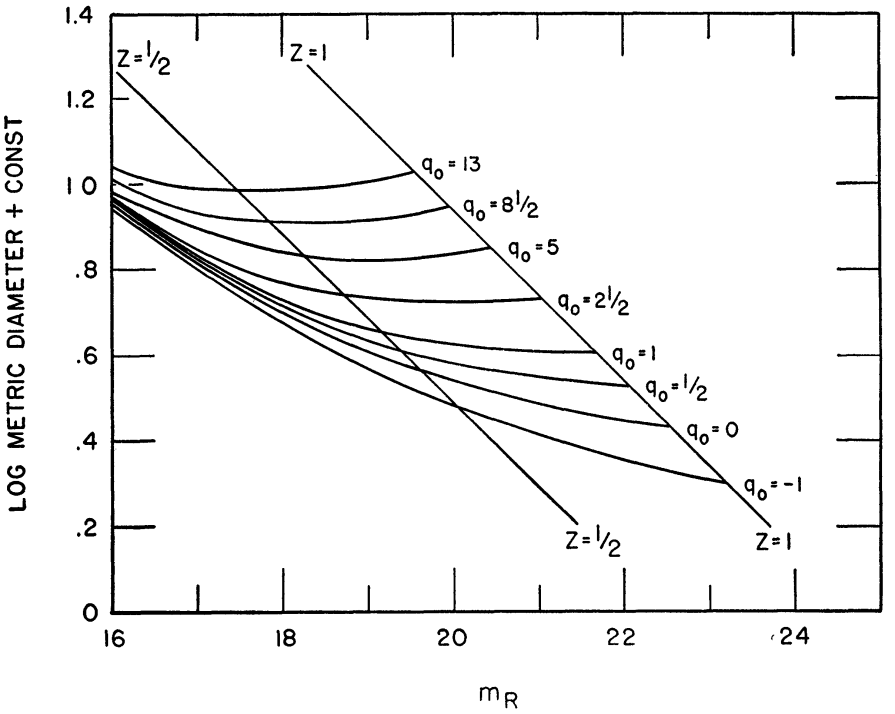


FIG 8.—Same as Fig. 7 but with the $k_R$ term applied to the abscissa. Lines of constant red shift of $z = 0\,5$ and $z = 1\,0$ are shown. The curves in this diagram are for *metric* diameters

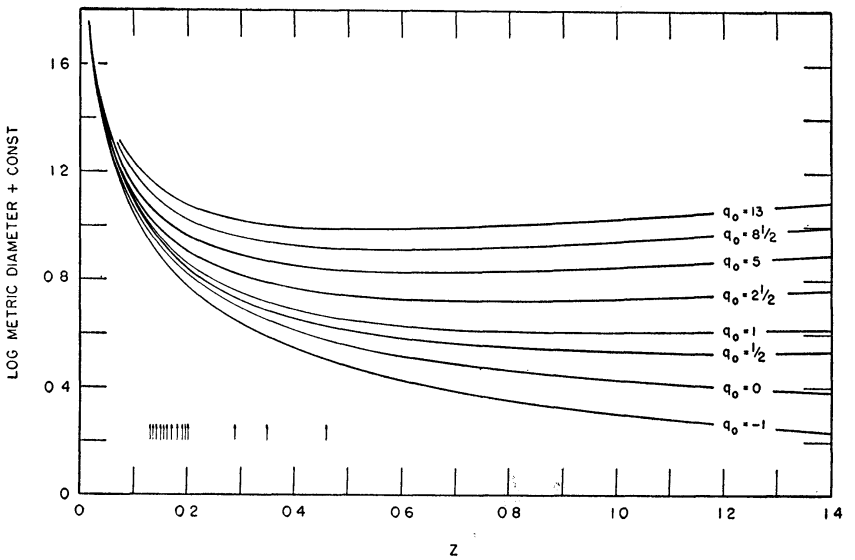


FIG. 9.—Same as Fig 8 but with the red shift as the independent variable. The arrows on the abscissa represent clusters whose red shifts have already been measured. The limit of the 200-inch telescope is probably near $z = 0.6$. The curves in this diagram are for *metric* diameters.

are three additional clusters with red shifts greater than $z = 0.2$. One is Minkowski's cluster 1409, +5224 with $z = 0.46$. The other two are Cl 0024 + 1654, and Cl 1447 + 2619 discovered by Humason and Sandage on the 48-inch Schmidt red sky-survey plates and confirmed with the 200-inch. Humason attempted red-shift measures on both but failed because of the bright night sky at the time of sunspot maximum. From his eight-color measurements Baum estimates their red shifts to be $z = 0.29$ and $z = 0.35$, respectively. The red shifts of these 13 clusters are marked as arrows in Figure 9 to indicate how far a test could now be carried, once operationally defined angular metric diameters are obtained.

To conclude this section it is important to point out a practical result of these calculations. *To avoid the aperture effect in measuring apparent magnitudes, it is incorrect to use measuring apertures whose size is inversely proportional to z, as would be the intuitive choice.* Apertures designed to give the same percentage of the total light for nearby and distant galaxies must follow the curves of Figure 9 given by equations (51) and (52). Unfortunately, this function depends on $q_0$, which is what we wish to find from the magnitude measures for the [$m$, $z$] relation [Sec. II]. However, the $m(r)$ function varies so slowly with $r$ for large $r$ (see HMS 1956, Appendix A, Fig. A2) that an iteration process can be performed in practice.

*b) Isophotal Diameters*

The diameters of galaxies determined from photographic plates usually refer to the sizes of the isophotal contours. Isophotal diameters behave differently from metric diameters because in an expanding universe the surface brightness is not constant with changing distance but varies as $(1 + z)^{-4}$. Let $y$ be the linear size of some part of a galaxy. The angular size, seen from a distant $\sigma(u)$, is given by equation (49). The apparent luminosity of this source of absolute candle power $L$ ergs/sec, is given by equation (17). The surface brightness is then

$$B = \frac{l}{\theta^2} = \frac{L}{4\pi y^2 (1 + z)^4} = \frac{\text{const.}}{(1 + z)^4}, \tag{53}$$

provided that $L/y^2$ is constant (i.e., we assume identical galaxies in the sample studied). Equation (53) is, of course, in contrast to the normal situation in laboratory physics, where the angular area and the apparent luminosity of an extended source decrease by the same factor as the distance increases, thus keeping the surface brightness constant.

Equation (53) holds for all expanding universes which obey equations (17) and (49) and is therefore valid for all values of $q_0$, including the steady state. The equation was first derived by Hubble and Tolman (1935) and has been largely forgotten. However, its importance for many cosmological problems has recently been emphasized by Stock and Schücking in their discussion of magnitudes determined from isophotal diameters (1957).

To obtain the isophotal diameters, consider the following thought experiment. Suppose that the angular size of the isophotal contours of M31 are known, viz., at a given angular distance $\theta_i$ from the nucleus, corresponding to linear distance $y_i$, the surface brightness $B_i$ is known. Take M31 to a large distance where the red shift is $z$. The surface brightness at linear distance $y_i$ will now be smaller than it was before by the factor of $(1 + z)^4$ from equation (53). Consequently, to find the region in the "distant" M31 where the surface brightness equals the original value of $B_i$, we must sample closer to the nucleus where the surface brightness in the nearby M31 is brighter by $(1 + z)^4$. Call the distance from the nucleus of this region $y_j$, which subtends an angle $\theta_j(z)$. The two surface brightnesses are related by $B_j(z) = B_i(0)$, where $B_j(0) = B_i(0)(1 + z)^4$. In other words, this equation states that the isophote at point $y_j$ in a galaxy of red shift $z$ equals the surface brightness at $y_i$ in an identical galaxy at rest, where $B_i$ and $B_j$ are related in the galaxy at rest by $(1 + z)^4$. These considerations show that *contours of*

*equal surface brightness move across the face of a galaxy toward the nucleus as z increases, making the isophotal diameters smaller than the metric diameters for* $z > 0$.

To find the exact relation between the metric diameter and the isophotal diameter, we take the distribution of surface brightness across the face of a typical E galaxy to be

$$B = \frac{B_0}{[(\theta/a) + 1]^2}, \tag{54}$$

as given by Hubble (1930). Here $a$ is a parameter angle fixing the scale. Consider now the isophotal angular diameter $\theta_i$ corresponding to a given surface brightness $B_i$. At faint isophotal contours, $B_i \ll B_0$ and therefore

$$\theta_i = a\sqrt{\frac{B_0}{B_i}} \tag{55}$$

to an excellent approximation. We take $B_i$ to be fixed by the technique of observation (e.g., we may wish the angular diameter of galaxies to an isophote of 25 mag/square

TABLE 7

ISOPHOTAL DIAMETERS ACCORDING TO EQUATION (56)*

| $m_R - k_R$ | log $\theta$ Isophotal | $m_R - k_R$ | log $\theta$ Isophotal |
|---|---|---|---|
| 8 0 | 2 903 | 16 0 | +1 303 |
| 8 5 | 2 803 | 16 5 | +1 203 |
| 9 0 | 2 703 | 17 0 | +1 103 |
| 9 5 | 2 603 | 17 5 | +1 003 |
| 10 0 | 2 503 | 18 0 | +0 903 |
| 10 5 | 2 403 | 18 5 | +0 803 |
| 11 0 | 2 303 | 19 0 | +0 703 |
| 11 5 | 2 203 | 19 5 | +0 603 |
| 12 0 | 2 103 | 20 0 | +0 503 |
| 12 5 | 2 003 | 20 5 | +0 403 |
| 13 0 | 1 903 | 21 0 | +0 303 |
| 13 5 | 1 803 | 21 5 | +0 203 |
| 14 0 | 1 703 | 22 0 | +0 103 |
| 14 5 | 1 603 | 22 5 | +0 003 |
| 15 0 | 1 503 | 23 0 | −0 097 |
| 15 5 | 1 403 | | |

* To obtain $z$ as argument use Table 1 for the $m_R - k_R = f(z, q_0)$ relation

sec of arc), and ask how $\theta_i$ varies with $z$. The central surface brightness $B_0$ varies with $2$ as given by equation (53). Further, it is clear that the parameter angle $a$ is not an isophotal diameter but is a metric diameter and is governed by equation (51) or (52); i.e., $a$ is the angle where the observed $B$ falls to a fixed fraction ($\frac{1}{4}$) of the central value. Substituting equations (51) and (53) in equation (55) and collecting constants give $\log \theta_i = \text{const.} - 0.2\, m - 0.5 \log B_i$. Taking $B_i$ to be fixed by circumstances of the observations and using equation (29) gives the required result that

$$\theta_i = \frac{\text{const.}}{A} \tag{56}$$

for all $q_0 \geq 0$. The analysis for the steady-state model proceeds by substituting equations (52) and (53) in equation (55). Equation (56) is again obtained if we remember from equations (23′) and (29) that $A = z(1 + z)$. *Thus the isophotal diameters vary with* $A^{-1}$ *for all models considered.* Table 7 gives $\theta_i$ computed from equation (56) with the

constant equal to 1. The table is arranged with $m_R - k_R$ as the argument. If $z$ is used as argument, Table 1 for the $m_R - k_R = f(z)$ must be used. Note that all $q_0$ values lead to the same $\theta_i = f(m_R - k_R)$ relation because $m_R - k_R$ is a function of $A$ alone by equation (29). The log $\theta_i = f(A)$ function is shown in Figure 7 by the straight line. If we use $z$ as the independent variable, then $\theta_i = f(z)$ depends on $q_0$, and a separation between the models is obtained. This is because $z$ is a function of both $A$ and $q_0$ by equations (28). Equation (56) is therefore a function of both $z$ and $q_0$. The dependence of $q_0$ is shown in Figure 10, where log $\theta_i$ is plotted against $z$. This diagram should be compared with its analogue in Figure 9 for the metric angular diameter. As expected, for a given $z$

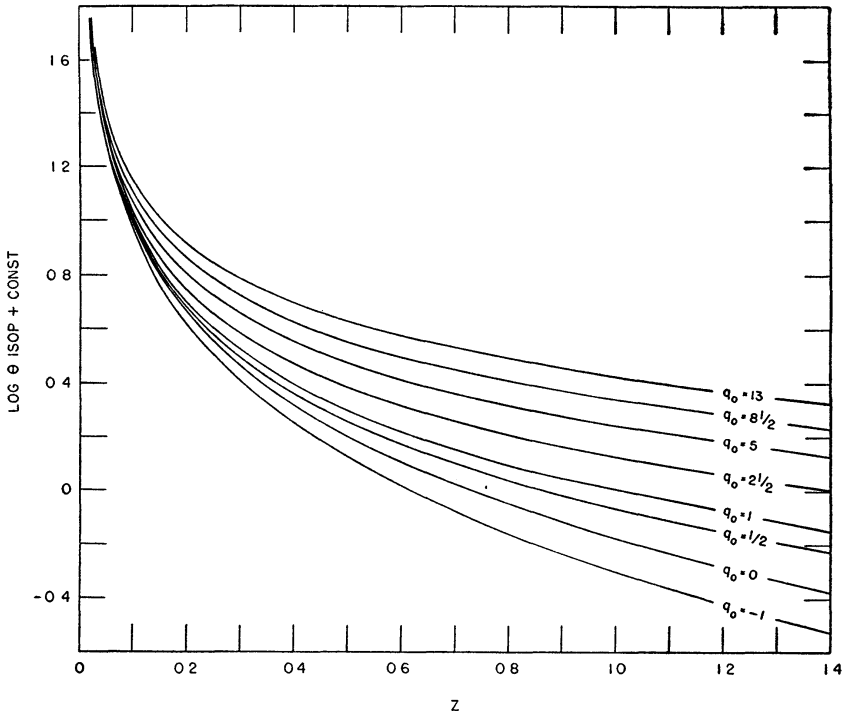


FIG 10.—The *isophotal* diameters as a function red shift Note that no minimum occurs in the curves. *Isophotal* diameters differ from *metric* diameters in this respect

the isophotal diameter is always smaller than the metric diameter for the reasons previously given. *It should also be noted from Table 7 and Figure 10 that θ (isophotal) has no minimum value at a finite* z *as does θ (metric) but approaches zero as* $z \to \infty$. Thus Hoyle's suggestion to use the minimum feature of angular diameters to decide between the steady-state model and exploding models with $\Lambda = 0$ does not apply to $\theta$ (isophotal) but only to $\theta$ (metric).

### *c) Application of Isophotal Diameters*

At a first glance the practical determination of isophotal diameters would appear to be quite simple. If a series of photographic plates with identical exposure times were taken on the same night of various clusters with different $z$ values and if the fog background of the sky was constant, then diameters of the galaxies measured visually on the plates would be isophotal. But unfortunately these measured diameters could not be compared directly with the predictions of Figure 10 because the photometric $k$ term enters the observational data, whereas the predictions refer to monochromatic isophotes.

Suppose the observations are made with red plates such as Eastman 103*a*-F behind a

Schott RG 2 filter ($\bar{\lambda} \approx 6800$ A). The observations of nearby galaxies with small $z$ will give isophotes for a wave length centered at $\lambda = 6800$ A. But for galaxies with $z = 0.5$, the observed isophotes refer to radiation *originating at* $\lambda_0 = 4540$ A, and because the energy distribution, $I(\lambda)$, varies with $\lambda$, this wave-length shift introduces a variation in the intrinsic intensity of the source. To correct for this $k$-term effect, we must know not only $I(\lambda)$ but also $B(\theta)$ by equation (54). The correction can be made as follows.

Suppose we measure the angular diameter to an observed surface brightness of $B_i = 22.0$ mag/$\square''$ at a fixed *monochromatic wave length of 6800 A* determined by the detector. Consider two identical galaxies, one at rest with $z_1 = 0$ and the other with a red shift $z_2 = 0.5$. Assume that the observed angular diameters at this isophote are $\theta_1(z = 0)$ and $\theta_2(z = 0.5)$. As mentioned above, the radiation of galaxy 2 that is observed at $\lambda = 6800$ A originated at $\lambda = 4540$ A. It is known that the energy distribution curve gives I(4540) > I(6800) for normal E galaxies with the effect that, if observations are confined to a wave length of 6800 A, galaxy 2 is brighter than it should be by the ratio I(4540)/I(6800) for equation (56) to apply. For the present illustration, suppose I(4540)/I(6800) = 2 (which is 0.75 mag.). To correct for this type of $k$ term we must move out on the face of galaxy 2 to an angle where the surface brightness is 0.75 mag. fainter than that observed at angle $\theta_2$. Equation (55) gives the correction to the observed angle $\theta_2$ as $\theta_2$ (corrected)/$\theta_2$ (observed) = $\sqrt{2}$. Note that $a$ and $B_0$ cancel in equation (55). Note also that for a positive $k$ term, the corrected angular diameter will always be larger than the isophotal diameter observed at a fixed wave length.

Corrections could be computed and applied to Figure 10 to obtain a prediction of the observed isophotal angles as a function of $z$. But the functions $I(\lambda)$, $k(z)$, and $B(\theta)$ must be known accurately. Until observations of $I(\lambda)$ by J. B. Oke are finished, it is premature to compute the corrections. But to summarize this section: *corrections for the* k *term must be applied to any observed isophotal diameters before comparison with equation* (56) *can be made.*

Stock and Schücking (1957) were probably the first to realize the nature of the corrections.

## V. THE TIME SCALE

A fourth possible test concerns the time scale. For exploding cosmologies of the type considered here ($\Lambda = 0$, pressure term = 0), equation (3) shows that a singular point $R(t_0) = 0$ exists in the finite past. This point is taken as the time of "creation" of the universe in its present cycle of expansion. In contrast, the steady-state theory requires that $R(t) = 0$ only at $t = \rightarrow - \infty$ (see eq. [19]), which means that there was no time in the finite past when the singular event $R(t) = 0$ occurred. The test between the theories concerns the possible elimination of all exploding models with $\Lambda = 0$ if they lead to an inadequately short time scale. Obviously,

$$t_0 \equiv \text{time since beginning of the present expansion cycle} \geq \text{age of the oldest stars} \quad (57)$$

must hold for any rational cosmology, and if the inequality is definitely violated by any model, then that model must be incorrect.

### *a) Exploding Models with $\Lambda = 0$, $p = 0$*

It will be shown presently that $t_0$ for exploding models is a function of $H_0^{-1}$ and $q_0$ alone. That this might be so is suggested by Figure 11, which schematically plots $R = f(q_0, t)$ obtained by the integration of equation (3). Three cases of $q_0$ are shown: (1) $q_0 = 0$, which requires $k = -1$, $\rho_0 = 0$, and $R(t) = ct$; (2) $q_0 = \frac{1}{2}$, which is the Euclidean case with $k = 0$ and $R(t) \propto t^{2/3}$; and (3) $q_0 > \frac{1}{2}$, which requires $k = +1$ and $R(t)$ is the curve of a cycloid. The vertical line in Figure 11 represents the present epoch of observation, $t_0$. The Hubble time $H_0^{-1}$ can be found from the following well-known construction.

Draw a tangent line to the curve at $R(t_0)$ and extend it back until it intersects the $t$-axis. Equation (4) requires that the distance from $t_0$ to this intersection is $H^{-1}$. For $\ddot{R} < 0$, which all Friedman models with $\Lambda = 0$ require, it is seen that $H^{-1}$ is always *greater* than the "age of the universe," $t_0$, except for the case of $q_0 = 0$, for which $t_0 = H^{-1}$. The function $t_0 = f(H_0^{-1}, q_0)$ is now found by integrating equation (3).

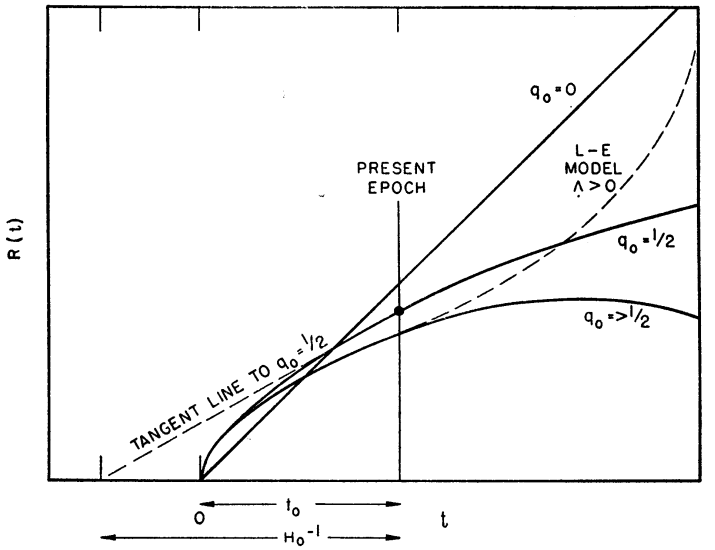


FIG 11.—The $R(t)$-curves for three cases of exploding models with $\Lambda = 0$ and for a generalized Lemaitre-Eddington model The relation between $H_0^{-1}$ and $t_0$ is obtained by the construction described in the text The curves are schematic

1. *The case* $k = +1$, $q_0 > \frac{1}{2}$.—This model corresponds to a closed universe of finite volume. Equation (3), with the dependence of $\rho(t)$ on $R(t)$ taken as $\rho(t) = Q/R^3(t)$ becomes

$$\dot{R} = \sqrt{\left(\frac{8\pi GQ}{3R} - c^2\right)} \tag{58}$$

or

$$\int_0^{t_0} dt = \int_0^{R_0} \frac{RdR}{\sqrt{[(8\pi GQ/3)R - c^2R^2]}}, \tag{59}$$

which integrates to

$$t_0 = \frac{8\pi GQ}{6c^3}\left[\sin^{-1}\left(\frac{6c^2R_0}{8\pi GQ} - 1\right) + \frac{\pi}{2}\right] - \frac{1}{c^2}\sqrt{\left(\frac{8\pi GQR_0}{3} - c^2R_0^2\right)}. \tag{60}$$

This conveniently reduces to a function of $H_0$ and $q_0$ alone by substituting equations (10′), (9), and (4) in equation (60), giving

$$H_0t_0 = \frac{1}{1-2q_0} + \frac{q_0}{(2q_0-1)^{3/2}}\left[\frac{\pi}{2} + \sin^{-1}\left(\frac{q_0-1}{q_0}\right)\right] \quad \text{for } k = +1 \tag{61}$$
$$q > \tfrac{1}{2}.$$

2. *The case* $k = 0$, $q_0 = \frac{1}{2}$.—For this model, equation (3) integrates to the well-known expression

$$R^{3/2} = \frac{3}{2}\sqrt{\left(\frac{8\pi GQ}{3}\right)}\, t. \tag{62}$$

Substitution of $\dot{R}_0 = \sqrt{(8\pi GQ/3R_0)}$, and $H_0 = \dot{R}_0/R_0$ into equation (62) gives

$$H_0 t_0 = \tfrac{2}{3} \, . \tag{63}$$

3. *The case* $k = -1$, $0 \leq q_0 < \tfrac{1}{2}$.—A similar calculation for these models gives

$$t_0 = \frac{1}{c^2}\sqrt{\left(\frac{8\pi GQ}{3}R_0 + R_0^2 c^2\right)} - \frac{8\pi GQ}{6c} \times \left\{\ln\left[\sqrt{\left(\frac{8\pi GQ}{3}R_0 + R_0^2 c^2\right)} + Rc + \frac{8\pi GQ}{6c}\right] - \ln\frac{8\pi GQ}{6c}\right\}, \tag{64}$$

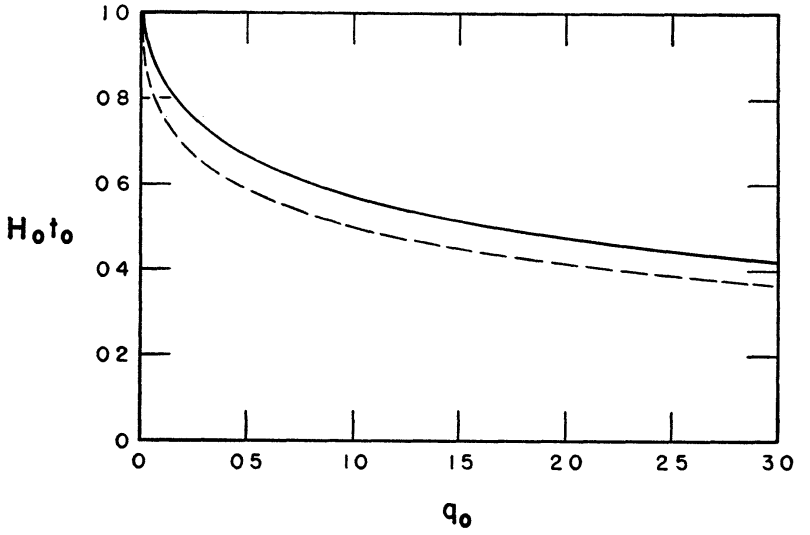


FIG 12.—The relation between $H_0t_0$ and $q_0$. The solid curve is for a universe where the pressure term is zero The dotted curve is for a radiation-filled universe where radiation pressure dominates.

which again reduces to a function of $q_0$ alone by substituting equations (3), (9), and (4) into equation (64), giving

$$H_0 t_0 = \frac{1}{1-2q_0} - \frac{q_0}{(1-2q_0)^{3/2}} \ln\left[\frac{1-q_0}{q_0} + \frac{\sqrt{(1-2q_0)}}{q_0}\right] \quad \text{for } k = -1, \; 0 \leq q_0 < \tfrac{1}{2} \, . \tag{65}$$

Equations (61) and (65) are of obvious importance because the expansion time scale can be obtained, once observed values of $H_0$ and $q_0$ are available. Figure 12 shows $H_0t$ as a function of $q_0$ obtained from equations (61), (63), and (65), The data are given in Table 8. Notice that $H_0t_0$ never becomes greater than 1, which means that the time scale can be, at most, as long as $H^{-1}$ for exploding models with $\Lambda = 0$.

Equations (61), (63), and (65) are not valid near the beginning of the expansion because the pressure terms in the fundamental equations (2) and (3) cannot be neglected near $t_0 = 0$. When $R(t)$ is very much smaller than it is today, the radiation density dominates over the matter density, and the radiation pressure overpowers the density terms in equations (2) and (3), making the approximation that $p = 0$ invalid. It will now be shown that the estimates of the time scale by equations (61), (63), and (65) are not greatly in error by this fact.

*b) A Universe Filled with Radiation Only*

Consider a universe where the matter density is negligible compared with the radiation pressure term. This is the asymptotic model required by equation (3) near $t_0 = 0$. Some of the features of this model are discussed in the last paragraph of Section I. We require the time-scale equations.

For a radiation-filled model, the mass equivalent of the radiation density is given by $\rho = u/c^2$, where $u = aT^4$. The radiation pressure is $p = u/3$. The fundamental equations corresponding to equations (2) and (3) are, with $\Lambda = 0$,

$$\frac{\dot{R}^2}{R^2} + \frac{2\ddot{R}}{R} + \frac{8\pi GQ}{3c^2R^4} = -\frac{kc^2}{R^2}, \tag{66}$$

$$\frac{\dot{R}^2}{R^2} - \frac{8\pi GQ}{3c^2R^4} = -\frac{kc^2}{R^2}, \tag{67}$$

TABLE 8

TIME SCALE FOR DUST- AND RADIATION-FILLED UNIVERSES*

| $q$ | DUST UNIVERSE | | RADIATION UNIVERSE | |
|---|---|---|---|---|
| | $H_0t_0$ | $t_0$ ($10^9$ yr) | $H_0t_0$ | $t_0$ ($10^9$ yr) |
| 0 000 | 1 0000 | 13 00 | 1 0000 | 13 00 |
| 0 025 | 0 9350 | 12 16 | 0 8635 | 11 22 |
| 0 050 | 0 8981 | 11 67 | 0 8172 | 10 62 |
| 0 100 | 0 8465 | 11 00 | 0 7597 | 9 88 |
| 0 2 | 0 7787 | 10 12 | 0 6910 | 8 98 |
| 0 3 | 0 7319 | 9 51 | 0 6461 | 8 40 |
| 0 4 | 0 6960 | 9 05 | 0 6126 | 7 96 |
| 0 5 | 0 6667 | 8 67 | 0 5858 | 7 61 |
| 0 6 | 0 6423 | 8 35 | 0 5635 | 7 33 |
| 0 7 | 0 6209 | 8 07 | 0 5445 | 7 08 |
| 0 8 | 0 6022 | 7 83 | 0 5279 | 6 86 |
| 0 9 | 0 5857 | 7 61 | 0 5132 | 6 67 |
| 1 0 | 0 5708 | 7 42 | 0 5000 | 6 50 |
| 1 5 | 0 5133 | 6 67 | 0 4495 | 5 84 |
| 2 | 0 4728 | 6 15 | 0 4142 | 5 38 |
| 2 5 | 0 4420 | 5 75 | 0 3874 | 5 04 |
| 3 | 0 4173 | 5.42 | 0 3660 | 4 76 |
| 5 | 0 3515 | 4 57 | 0 3090 | 4 02 |
| 8 5 | 0 2897 | 3 77 | 0 2554 | 3 32 |
| 13 | 0 2457 | 3 19 | 0 2171 | 2 82 |

* $t_0$ computed with $H_0 = 75$ km/sec $10^6$ pc; $H_0^{-1} = 13 \times 10^9$ years

where the varation of $u(t)$ with $R$ is taken to be $u(t) = Q/R^4$, as explained in Section I. Recall further that

$$\frac{kc^2}{R_0^2} = H_0^2(q_0 - 1), \tag{14}$$

so that $q_0 = +1$ for $k = 0$; $q_0 > 1$ for $k = +1$; and $0 < q_0 < 1$ for $k = -1$.

1. *The case $k = +1$, $q_0 = 1$.*—For this model, equation (67) integrates to

$$t_0 = \frac{1}{c^2}\left[\sqrt{\left(\frac{8\pi GQ}{3c^2}\right)} - \sqrt{\left(\frac{8\pi GQ}{3c^2} - c^2R_0^2\right)}\right], \tag{68}$$

which can be simplified by using equations (67), (14), and $H_0 \equiv \dot{R}_0/R_0$, with the result that

$$H_0 t_0 = \frac{\sqrt{(q_0)} - 1}{q_0 - 1}. \tag{69}$$

This is the analogous expression to equation (61).

2. *The case $k = 0$, $q_0 = 1$ (the Euclidean model).*—Equation (67) easily integrates and simplifies to

$$H_0 t_0 = \tfrac{1}{2}, \tag{70}$$

which should be compared with equation (63).

3. *The case $k = -1$, $0 < q_0 < 1$.*—Equation (67) integrates to

$$t_0 = \frac{1}{c^2}\sqrt{\left(\frac{8\pi GQ}{3c^2} + c^2R_0^2\right)} - \frac{1}{c^2}\sqrt{\left(\frac{8\pi GQ}{3c^2}\right)}, \tag{71}$$

which simplifies in the same manner to

$$H_0 t_0 = \frac{1 - \sqrt{q_0}}{1 - q_0}. \tag{72}$$

Equation (72) is the analogue of equation (65).

The $H_0 t_0$ values computed from equations (69), (70), and (72) are given in Table 8 and shown in Figure 12 as a dotted line, so that a direct comparison with the models with $p = 0$ can be made. Note that the $H_0 t_0$ values for the pressure-dominant case are quite similar to those of the density-dominant case. Consequently, statements made by some authors that equations (61), (63), and (65) cannot be used to estimate the order of magnitude of $H_0 t_0$ because of the failure of the assumption $p = 0$ near $t_0 = 0$ appear to be incorrect.

To conclude this section it might be argued that the basis of this entire approach is fallacious because, in reality, $R(t)$ can never be zero due, among other things, to the possible net angular momentum of random motions and to the impossibility of the condition $\rho = \infty$. But it should be pointed out that $R(t)$ need not be zero to estimate the order of $H_0 t_0$ from these considerations. Equation (57) can be relaxed for this particular problem by changing the left side to read "the time since the formation of the galaxies." For this we need only to go back to a time when the density of the pre-condensed matter was equal to the present average density of a typical galaxy. This density is certainly smaller than $10^{-20}$ gm/cm$^3$. If the present mean density is of the order of $10^{-29}$ gm/cm$^3$, as obtained from equation (7′), $R$ must be taken back only a factor of $10^{-3}$ of its present value to attain a density increase of $10^9$. To this point, equations (2) and (3) or equations (66) and (67) are certainly valid and the methods of this section should be satisfactory.

### *c) Data Available on the Time Scale*

We now wish to see whether equation (57) is satisfied by any of the exploding models with $\Lambda = 0$. The present estimate of $H_0$ is 75 km/sec $10^6$ pc or $H^{-1} = 13.0 \times 10^9$ years (Sandage 1958). Furthermore, it is shown in Section II that $0 < q_0 < 3$ with the best current estimate as $q_0 = 1 \pm \frac{1}{2}$. Consequently, $k$ must be $+1$ and $H_0 t_0 = 0.571 \pm 0.1$. Therefore, the left side of equation (57) is $t_0 = 7.4 \times 10^9$ years, while the right side is estimated to be greater than $20 \times 10^9$ years when the latest stellar models computed by Hazelgrove and Hoyle (1959) are applied to the observational data (O. C. Wilson for the oldest field stars; Sandage for NGC 188; Arp for M5).

Thus equation (57) appears to be violated by about a factor of 3. This is probably not so convincing as it might first appear because (1) the value of $H_0$ may still be in error by

perhaps a factor of 2, and (2) the theory of age dating by stellar models is undoubtedly uncertain by a least this amount. It would seem to this writer that the greatest uncertainty must presently be placed on the stellar models and that the evolutionary time-scale problem must be solved before we eliminate exploding cosmologies because of equation (57).

But, for the moment, let us trace the consequence if equation (57) *is* violated. There are two ways to "save the phenomenon." The first is to adopt the steady-state theory where the left side of equation (57) is infinite. The second is to consider exploding models with $\Lambda > 0$. This last possibility is discussed in Section VI. Neither way is satisfactory because both models require $q_0 = -1$, whereas the observations show $q_0 \cong +1$. Thus, if the data leading to $q_0 = +1$ are taken seriously, we would be forced to conclude that *no cosmological models exist of the type here considered which will fit all data*—i.e., those models which give the correct deceleration parameter have too short a time scale, and the two models which give an acceptable time scale (steady state and exploding with $\Lambda > 0$) require $\ddot{R}$ to be positive. But the observations show that $\ddot{R} < 0$.

It is my opinion that for the moment it is better to assume that the observational data, together with estimates of $dL/dt$ and the Scott effect, are not well known rather than to claim that current cosmological theory is inadequate.

## VI. EXPLODING MODELS WITH $\Lambda > 0$

Model universes with $\Lambda > 0$ are general cases of the Lemaitre-Eddington type. The $R(t)$-curves begin like those for $\Lambda = 0$ in Figure 11, but, for sufficiently large $R$, the $\Lambda R$ term in equation (3) dominates. The asymptotic form for large $R$ is

$$\lim R(t) = \text{const.} \times \exp \sqrt{\frac{\Lambda}{3}}\, ct \qquad (t \to \infty) \ , \quad (73)$$

which is found directly from equation (3) if $k = 0$.

The time scale for these models depends upon $\Lambda$. As soon as $\ddot{R}$ becomes positive, $t_0$ becomes larger than $H_0^{-1}$. The time $t_0$ can be made as long as desired by changing the value of $\Lambda$, as is seen from Figure 11.

The general property of the models is that they approach, in the limit, the steady-state model. That is, $q_0 = -1$ for the $R(t)$ given by equation (73). This is unfortunate because the tests based on the $q_0$ value described in Sections III, IV, and V are therefore not unique. *If observations show* $q_0$ *to be* $-1$, *we cannot decide between a steady-state universe and a Lemaitre-Eddington universe.* The only test between the two would be to look for the effects of aging in the far reaches of space. If the mean parameters of distant galaxies were found to be systematically different from those of nearby galaxies, then the "perfect cosmological principle," necessary for the steady-state model, would be violated. But to pursue the available observational data is beyond the scope of this paper. It suffices to say that no uncontested evidence is presently available for either side.

It is a pleasure to thank H. P. Robertson for reading and commenting on the manuscript. It is also a pleasure to thank my wife for several useful discussions. Special thanks are due to Fred Hoyle, for many helpful conversations and discussions

## APPENDIX A

### EQUATIONS FOR $(z, A)$ AND $N(m, q_0)$ FOR COUNTS OF FIELD GALAXIES

For the sake of completeness, the explicit equations for $[m, z, q_0]$, and $N(m, q_0)$ are given, together with the asymptotic values for $N(m, q_0)$ The function $A$ is defined by

equation (29) with $C = 22.516$. The function $P$ is defined by equation (31). To simplify the notation we denote $m_R - k_R$ by $m$ in the following:

$q_0 = -1$ (*steady state*):

$$z = \frac{-1 + \sqrt{(1+4A)}}{2}, \tag{A1}$$

$$\log N(m) = \log\left[\ln(1+z) - \frac{z(2+3z)}{2(1+z)^2}\right] + 5.77794, \tag{A2}$$

$$\lim \log N(m) = \lim \log [\ln \sqrt{A}] = \infty \qquad (A \to \infty,\ m \to \infty). \tag{A3}$$

$q_0 = 0$:

$$1 + z = \sqrt{(1+2A)}, \tag{A4}$$

$$\log N(m) = \log [P\sqrt{(1+P^2)} - \sinh^{-1} P] + 5.47570, \tag{A5}$$

$$\lim \log N(m) = \infty \qquad (m \to \infty). \tag{A6}$$

$q_0 = \frac{1}{2}$ (*Euclidean*):

$$1 + z = \frac{1 + A + \sqrt{(1+2A)}}{2}, \tag{A7}$$

$$\log N(m) = 3 \log A - 3 \log\left[\frac{1 + A + \sqrt{(1+2A)}}{2}\right] + 5.29960, \tag{A8}$$

$$\lim \log N(m) = \log N(m)_{\max} = 5.29960 + 3 \log 2 = 6.20269 \quad (A \to \infty). \tag{A9}$$

$q_0 = 1$:

$$z = A, \tag{A10}$$

$$\log N(m) = \log [\sin^{-1} P - P\sqrt{(1-P^2)}] + 5.47570, \tag{A11}$$

$$\lim \log N(m) = \log N(m)_{\max} = 5.47570 + \log \frac{\pi}{2} = 5.67182 \quad (A \to \infty). \tag{A12}$$

$q_0 = 2.5$:

$$1 + z = 2.5(1 + A) - 1.5\sqrt{(1+2A)}, \tag{A13}$$

$$\log N(m) = \log [\sin^{-1} P - P\sqrt{(1-P^2)}] + 4.57261, \tag{A14}$$

$$\lim P = 0.8 \qquad (A \to \infty). \tag{A15}$$

$$\lim \log N(m) = 4.22320 \qquad (A \to \infty), \tag{A16}$$

$$\lim \log N_c(m) = 5.00306 \qquad (A \to \infty), \tag{A17}$$

$$\log N(m)_{\max} = 4.57261 + \log \frac{\pi}{2} = 4.76873. \tag{A18}$$

$q_0 = 5$:

$$1 + z = 5(1 + A) - 4\sqrt{(1+2A)}, \tag{A19}$$

$$\log N(m) = \log [\sin^{-1} P - P\sqrt{(1-P^2)}] + 4.04434, \tag{A20}$$

$$\lim P = 0.6 \qquad (A \to \infty), \tag{A21}$$

$$\lim \log N(m) = 3.25786 \qquad (A \to \infty)\,, \tag{A22}$$

$$\lim \log N_c(m) = 4.51827\,, \tag{A23}$$

$$\log N(m)_{\max} = 4\ 04434 + \log \frac{\pi}{2} = 4.24046\,. \tag{A24}$$

$q_0 = 8.5$:

$$1 + z = 8.5\,(1 + A) - 7.5\sqrt{(1 + 2A)}\,, \tag{A25}$$

$$\log N(m) = \log [\sin^{-1} P - P\sqrt{(1 - P^2)}] + 3.66952\,, \tag{A26}$$

$$\lim P = 0.470588 \qquad (A \to \infty)\,, \tag{A27}$$

$$\lim \log N(m) = 2.54303 \qquad (A \to \infty)\,, \tag{A28}$$

$$\lim \log N_c(m) = 4.15622 \qquad (A \to \infty)\,. \tag{A29}$$

$$\log N(m)_{\max} = 3.66952 + \log \frac{\pi}{2} = 3.86564\,. \tag{A30}$$

$q_0 = 13$:

$$1 + z = 13(1 + A) - 12\sqrt{(1 + 2A)}\,, \tag{A31}$$

$$\log N(m) = \log [\sin^{-1} P - P\sqrt{(1 - P^2)}] + 3.37879\,, \tag{A32}$$

$$\lim P = 0.384615 \qquad (A \to \infty)\,, \tag{A33}$$

$$\lim \log N(m) = 1.97825 \qquad (A \to \infty)\,, \tag{A34}$$

$$\lim \log N_c(m) = 3.87041 \qquad (A \to \infty)\,, \tag{A35}$$

$$\log N(m)_{\max} = 3.37879 + \log \frac{\pi}{2} = 3.57491\,. \tag{A36}$$

When it exists, the quantity $N(m)_{\max}$, multiplied by $Q = 41253$, gives the total number of galaxies in the universe for the various models.

## REFERENCES


Alpher, R. A. 1948, *Phys. Rev.*, **74**, 1577.
Alpher, R. A., and Herman, R. C 1949, *Phys. Rev.*, **75**, 1089
Baum, W. A. 1957, *A.J.*, **62**, 6.
Bergh, S. van den. 1957, *Zs. f. Ap.*, **43**, 236.
Bondi, H 1952, *Cosmology* (Cambridge: Cambridge University Press).
Bondi, H., and Gold, T. 1948. *M N.*, **108**, 252.
Code, A D. 1959, *Pub. A S.P.*, **71**, 118.
Davidson, W. 1959, *M.N.*, **119**, 54.
Dunham, T. 1939, *Proc Amer. Phil Soc.*, **81**, 277.
Eddington, A. S 1930, *Internal Constitution of the Stars* (Cambridge: Cambridge University Press), p 371.
Friedman, A. 1922, *Zs f Phys*, **10**, 377.
Heckmann, O 1942, *Theorien der Kosmologie* (Berlin).
Holmberg, E. 1957, *Medd. Lunds Obs*, Ser. II, No. 136.
Hoyle, F. 1959, *Paris Symposium on Radio Astronomy* (Stanford Calif : Stanford University Press), p. 529.
Hoyle, F., and Sandage, A 1956, *Pub. A.S.P.*, **68**, 301.
Hubble, E. 1926, *Ap. J.*, **64**, 321.
——— 1929, *Proc. Nat. Acad. Sci.*, **15**, 168.
——— 1930, *Ap. J.*, **71**, 231.
——— 1936*a*, *The Realm of the Nebulae* (New Haven: Yale University Press)
——— 1936*b*, *Ap J*, **84**, 158.
——— 1936*c*, *ibid*, p 270
——— 1936*d*, *ibid*, p 517
———. 1953, *M N*, **113**, 658.

Hubble, E., and Humason, M. L. 1931, *Ap J.*, **74**, 43.
Hubble, E , and Tolman, R. 1935, *Ap J.*, **82**, 302.
Humason, M. L. 1931, *Ap. J.*, **74**, 35.
———. 1936, *ibid.*, **83**, 10.
Humason, M. L., Mayall, N. U., and Sandage, A. R. 1956, *A.J.*, **61**, 97.
McCrae, W. H. 1953, *Report on Progress in Physics* (London: Physical Society), **16**, 321
McVittie, G. C. 1956, *General Relativity and Cosmology* (London: Chapman & Hall).
Mattig, W. 1958, *A.N.*, **284**, 109.
———. 1959, *ibid.*, **285**, 1.
Minkowski, R. 1960, *Ap. J.*, **132**, 908.
Oort, J H. 1958, *La Structure et l'évolution de l'univers* (Brussels: Solvay Conference), p 163.
Robertson, H. P. 1928, *Phil. Mag.*, **5**, 845.
———. 1929, *Proc. Nat Acad. Sci.*, **15**, 822.
———. 1933, *Rev. Mod. Phys.*, **5**, 62.
———. 1938, *Zs f. Ap.*, **15**, 69.
——— 1955, *Pub. A.S.P.*, **67**, 82.
———. 1956, *Helvet. Phys. Acta*, Suppl. IV, p. 128
Salpeter, E. E. 1959, *Ap. J.*, **129**, 608.
Sandage, A. 1958, *Ap. J.*, **127**, 513.
Schmidt, M. 1959, *Ap. J.*, **129**, 243.
Scott, E. L. 1957, *A.J.*, **62**, 248.
Sitter, W. de 1933, *The Astronomical Aspect of the Theory of Relativity* (Berkeley: University of California Press).
Stebbins, J , and Whitford, A. E. 1948, *Ap. J* , **108**, 413
Stebbins, J., Whitford, A. E , and Johnson, H. L. 1950, *Ap J* , **112**, 469
Stock, J., and Schücking, E. 1957, *A.J.*, **62**, 98.
Walker, A. G. 1936, *Proc. London Math Soc.*, **42**, 90.
Wheeler, J. A. 1958, *La Structure et l'évolution de l'univers* (Brussels: Solvay Conference), p. 97.
Whitford, A E. 1954, *A.J.*, **59**, 194.
——— 1956, *ibid* , **61**, 353